20th ORAP Forum "High Performance Computing"

MULTISCALE ANALYSIS FOR ITER SUPERCONDUCTING COILS AND TUNNEL BEHAVIOUR DURING FIRES: TWO COMPUTING INTENSIVE MULTIDISCIPLINARY PROBLEMS

Bernhard Schrefler

University of Padua

December 13, 2006, PARIS

MULTISCALE ANALYSIS FOR ITER SUPERCONDUCTING COILS AND TUNNEL BEHAVIOUR DURING FIRES: TWO COMPUTING INTENSIVE MULTIDISCIPLINARY PROBLEMS

Bernhard A. Schrefler, Daniela P. Boso, F. Pesavento
Department of Structural and Transportation Engineering
Faculty of Engineering
University of Padua, ITALY

Marek Lefik, Dariusz Gawin
Chair of Geotechnical Engineering and Engineering Structures
Technical University of Łódz, POLAND

Ramon Codina, Javier Principe
International Centre for Numerical Methods in Engineering,
Technical University of Catalunya, UPC - Barcelona, Spain

International thermonuclear experimental reactor (ITER)

University of Padua

ITER will be built at Cadarache during the next 10 years and will operate for 20 years.

Overall cost is estimated in 10 GEuro: 50 % carried by the EU, the other 50% equally shared among China, India, Japan, Russia, South Korea, US.

In the ITER tokamak a plasma producing 500 MW from Deuterium Tritium reactions will be confined by a complex magnet system, composed of superconducting coils.

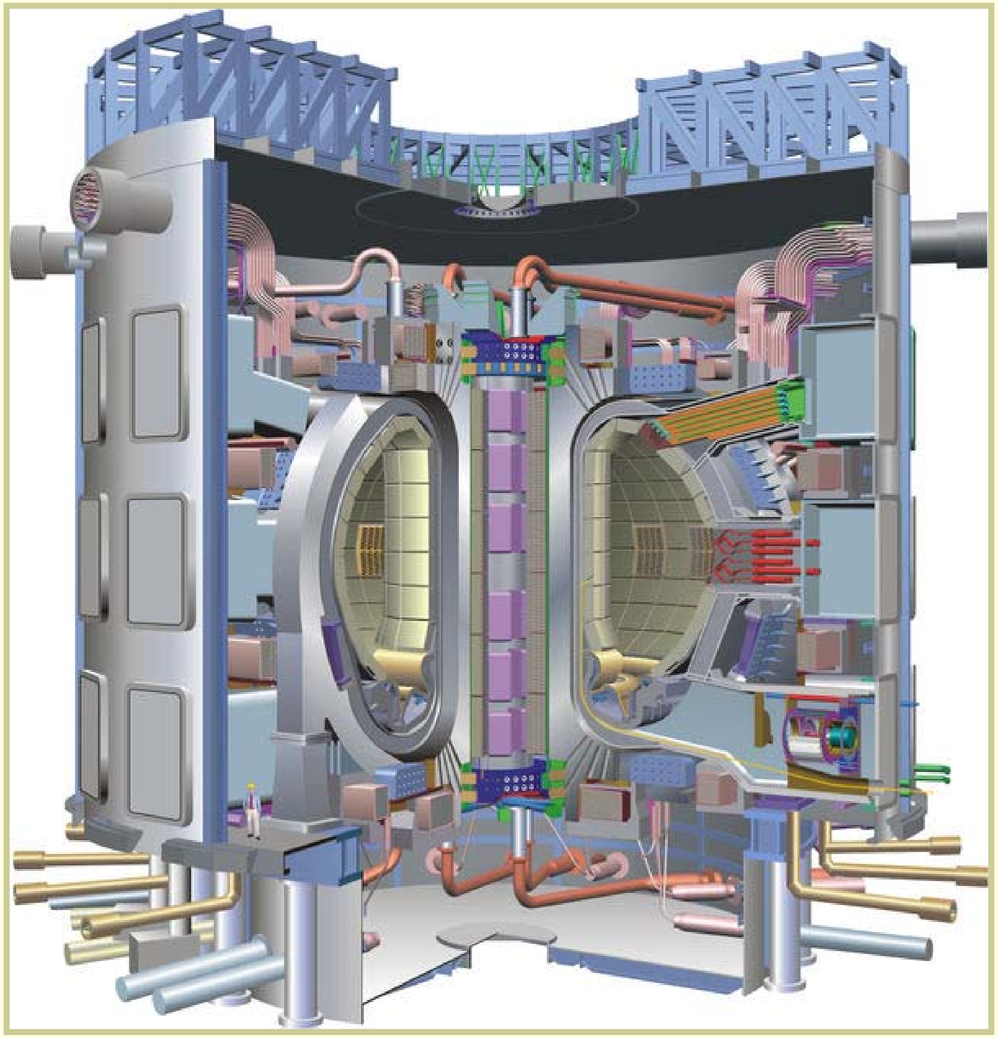

International thermonuclear experimental reactor (ITER)

ITER magnet structure consists of three main systems: a Central Solenoid coil (CS) composed of six modules, 18 Toroidal Field coils (TF), and 6 Poloidal Field coils (PF).

CS and TF coils will be manufactured using Nb3Sn based cables, while for the PF coils NbTi will be used.

All coils will be wound using cable-in-conduit conductors (CICC).

The magnet system, including the related cryogenics, will be the most expensive item in the whole ITER budget: up to 30 % of the total cost.

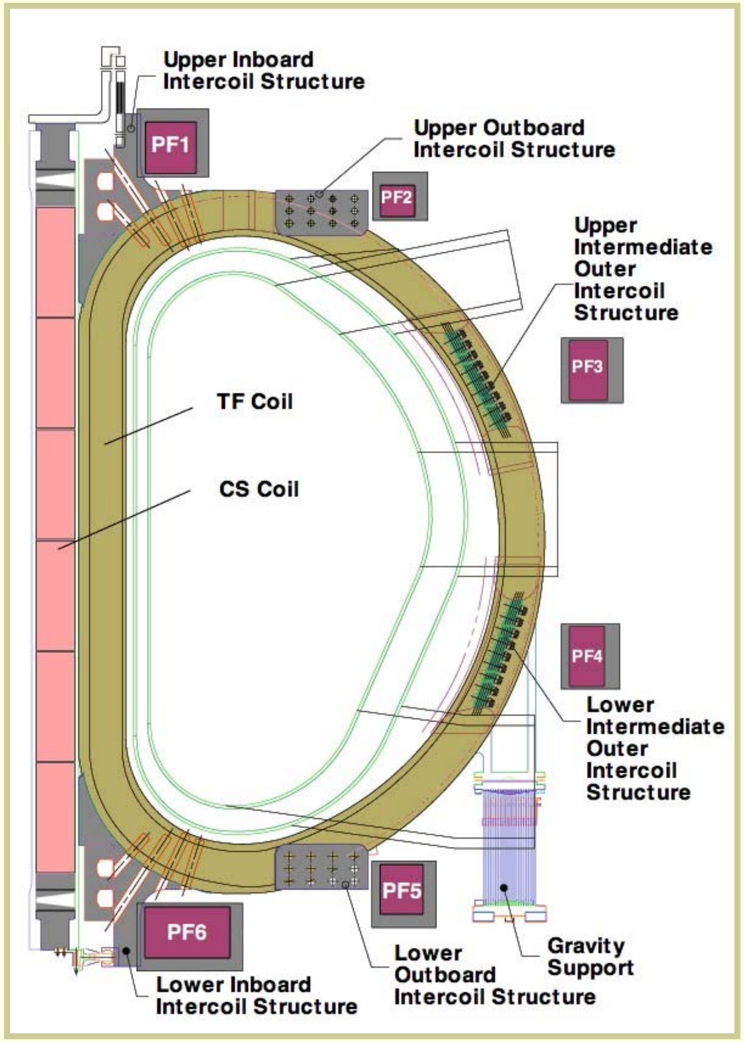

Multiscale modelling for composites including continuum to discrete linkage

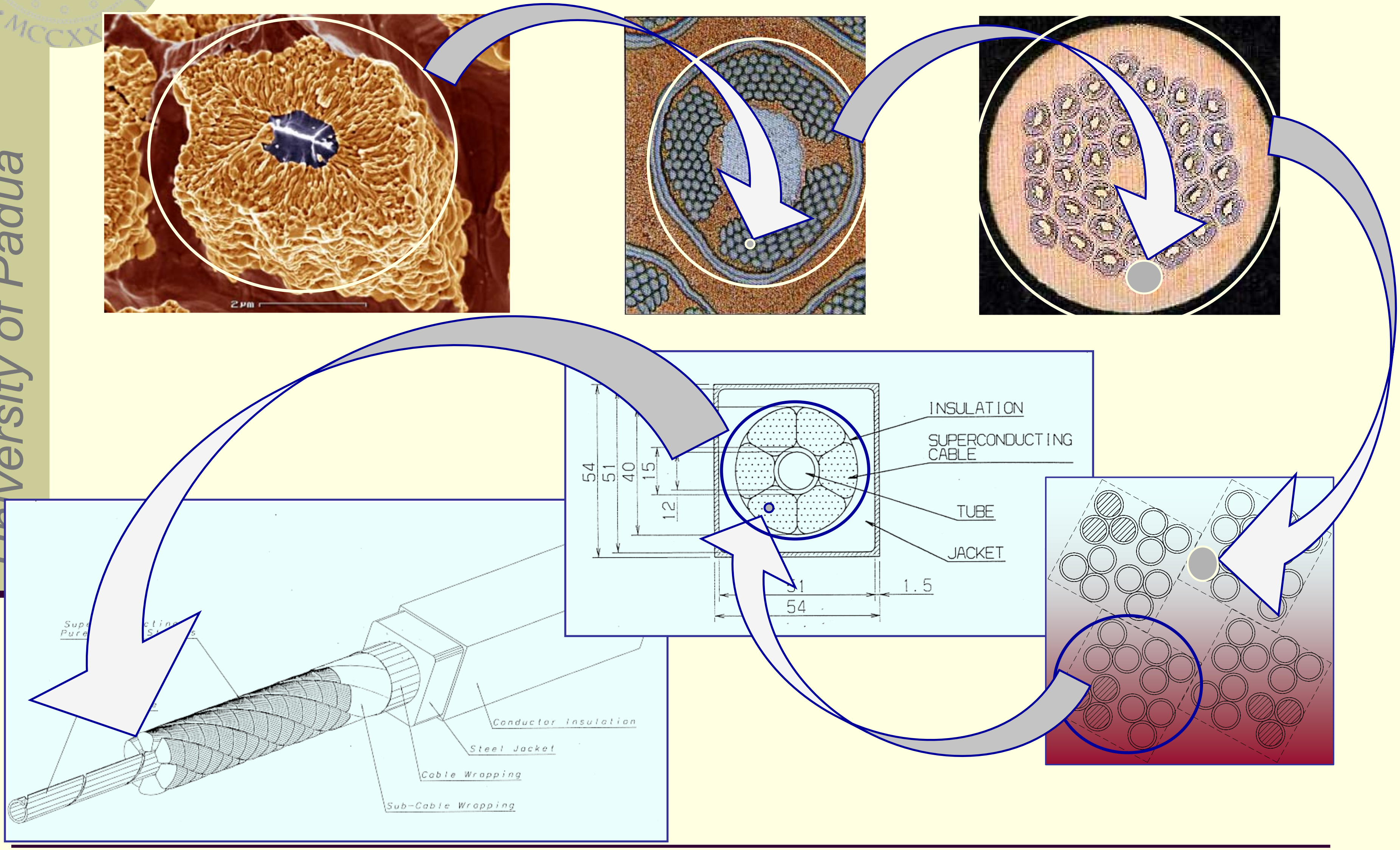

NB3SN multifilamentary composite wires

For practical applications, the superconductor is subdivided into fine filaments, which are twisted together and embedded in a low - resistivity matrix of normal metal (typically: bronze).

- The subdivision into fine filaments is required to eliminate instabilities in the superconductor known as flux jumps.
- The filament twisting is introduced to reduce inter-filament coupling when the wire is subjected to time-varying fields.
- The low- resistivity matrix is used as a current shunt in the case of a transition of the filaments to the normal resistive state, thereby limiting power dissipation and conductor heating (the resistivity of superconductors in the normal state is usually quite high).

Multiscale modelling for composites including continuum to discrete linkage

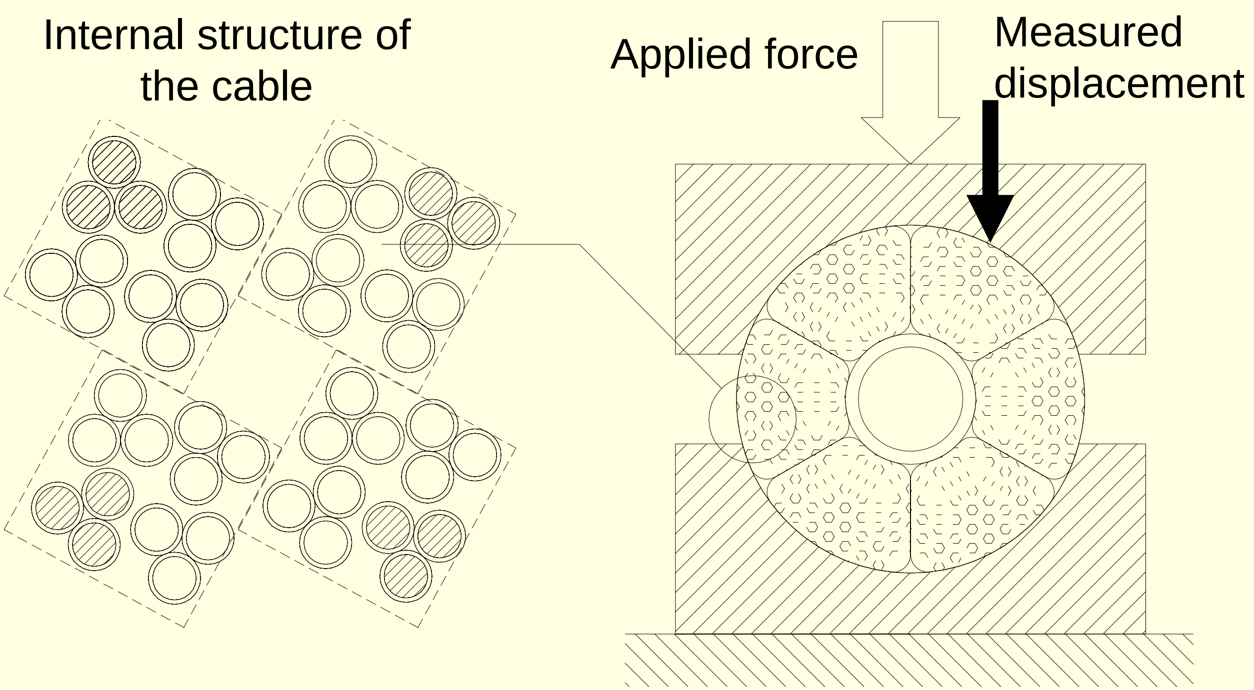

Scheme of a cell of the superconductor and a sketch of the experimental set-up of the university of Twente (Nijuhuis A & al. Mechanical and Electrical testing of an ITER CS1 Model Coil Conductor under Transverse Loading in a Cryogenic Press, Preliminary Report, University of Twente)

Multiscale modelling for composites including continuum to discrete linkage

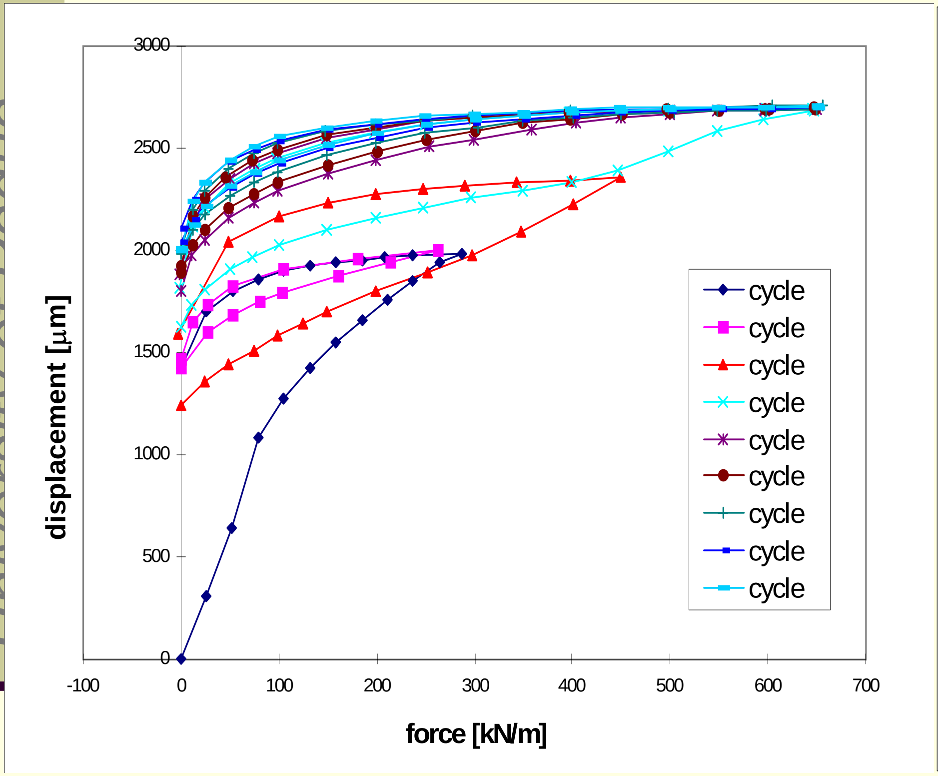

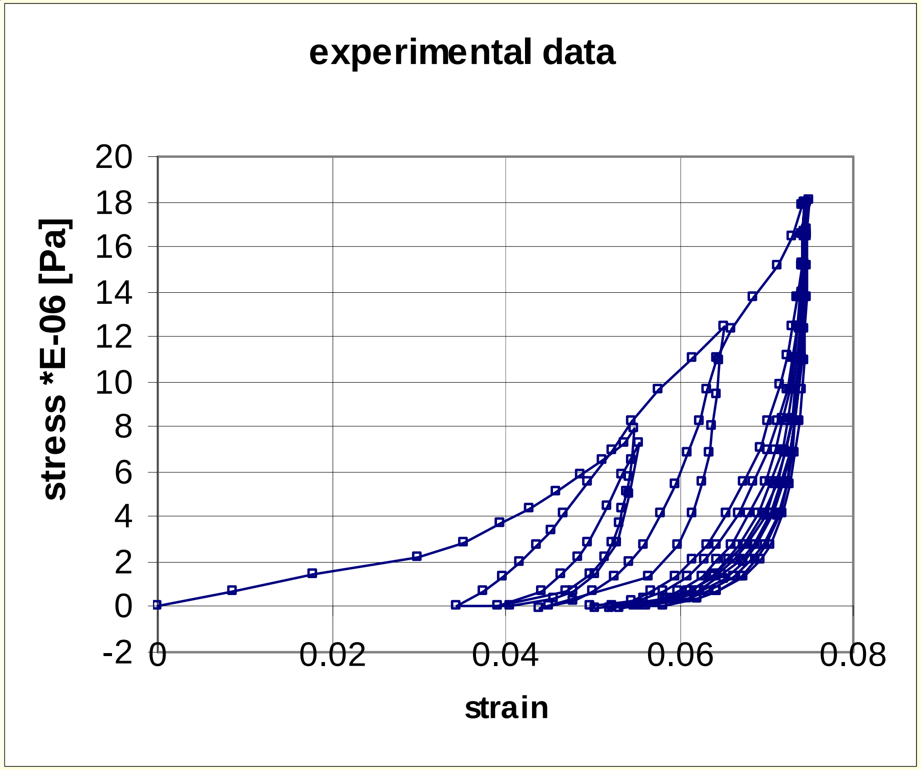

Force-displacement and equivalent stress-strain in the cable obtained in the experimental tests (University of Twente).

NB3SN multifilamentary composite wires

Nb_3Sn superconducting wires have a critical current density j_c that depends on the magnetic field, the temperature and the strain state ε of the superconductor

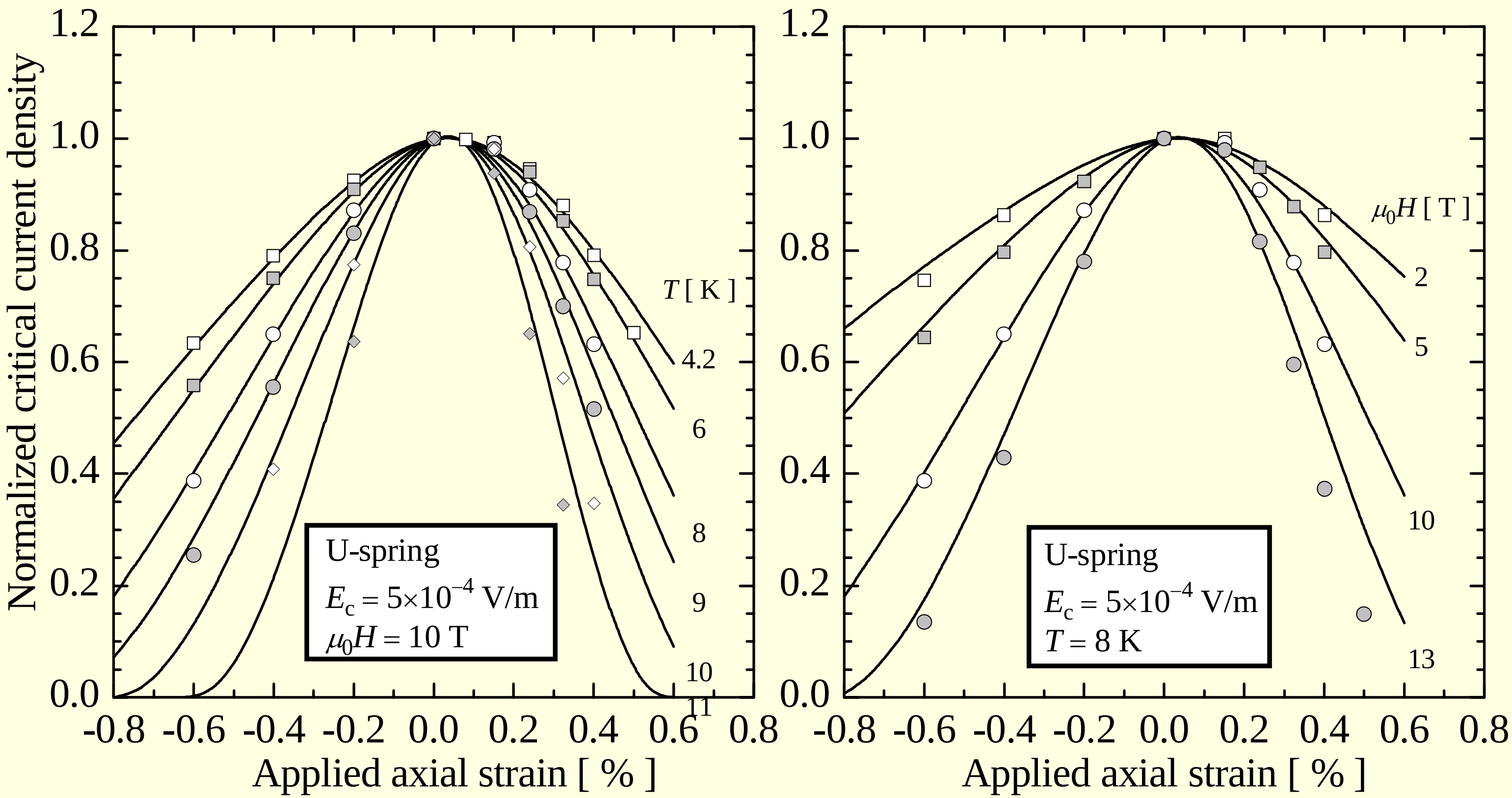

A. Godeke, *Performance Boundaries in Nb_3Sn Superconductors*, Ph.D. Thesis, University of Twente, 2005

FIRST THREE LEVELS

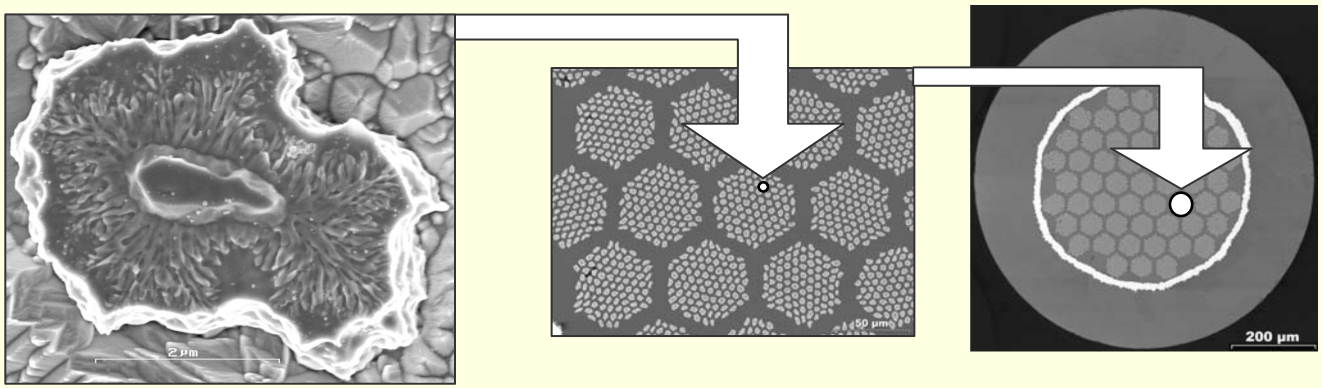

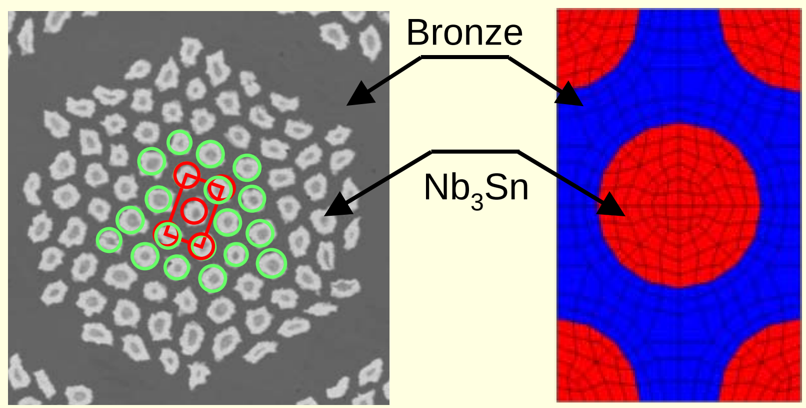

FIRST THREE LEVELS

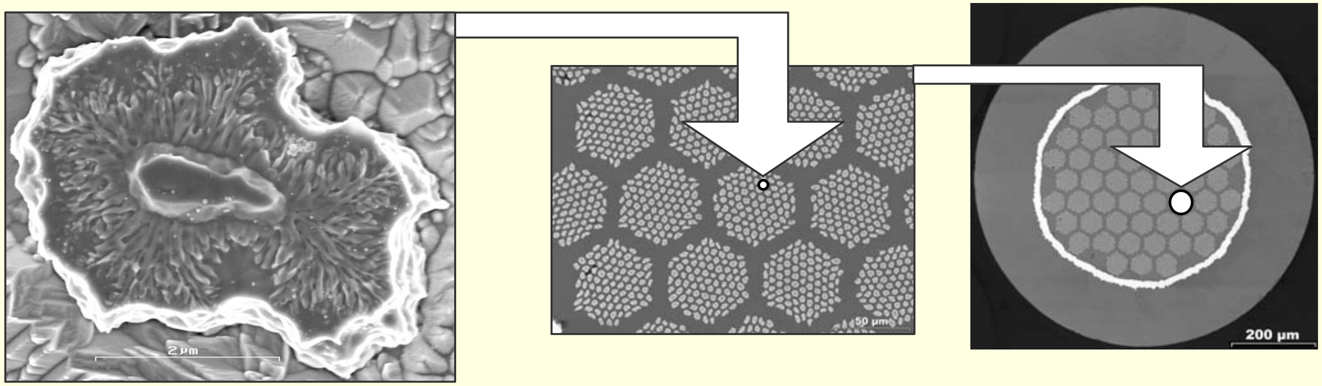

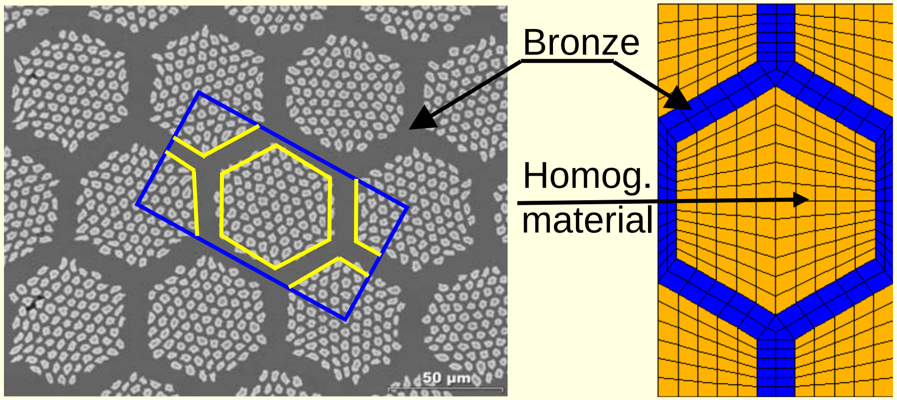

A three-scale model for EAS strands

Macro, meso and micro model

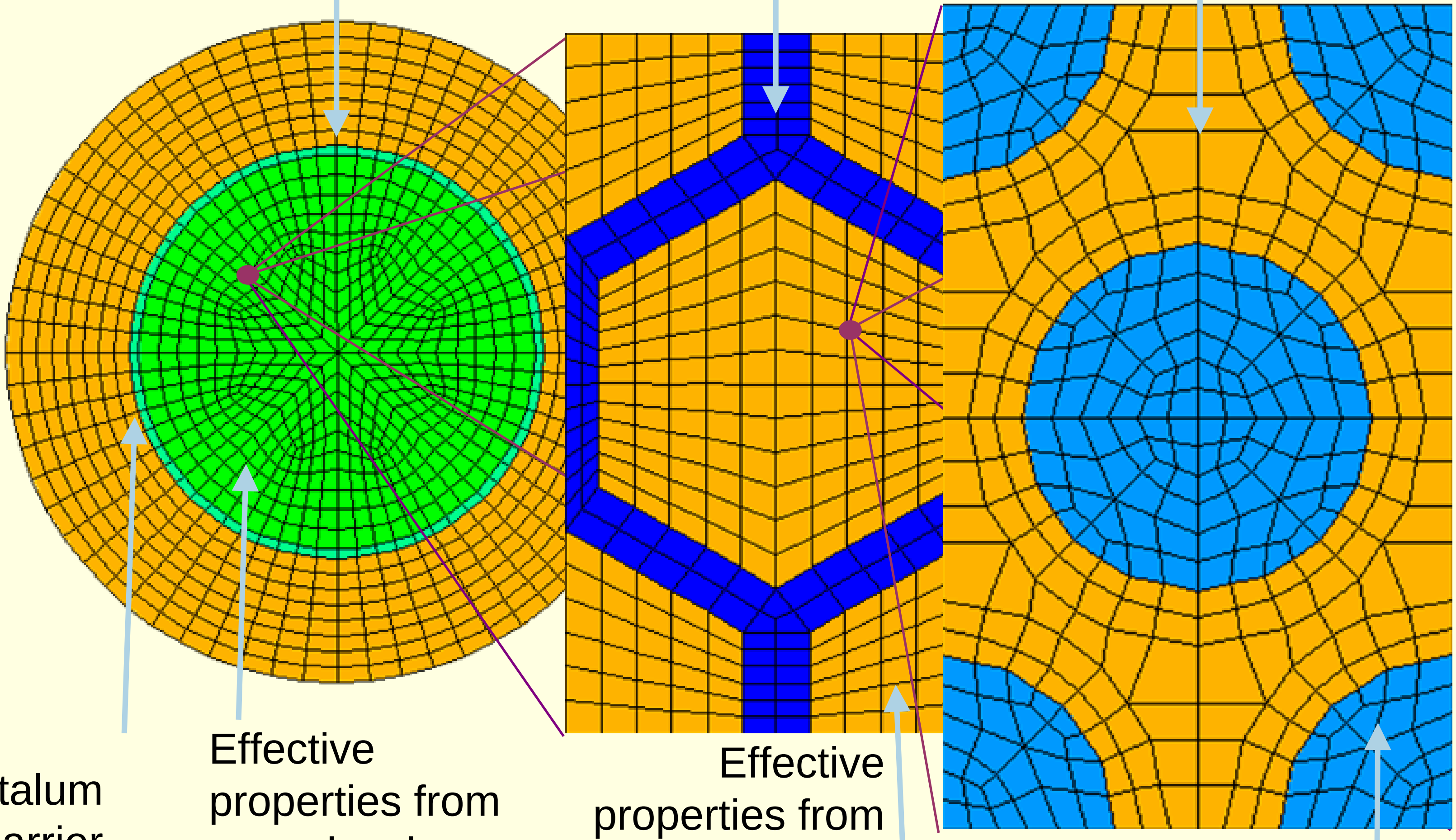

A three-scale model for EAS strands

University of Padua

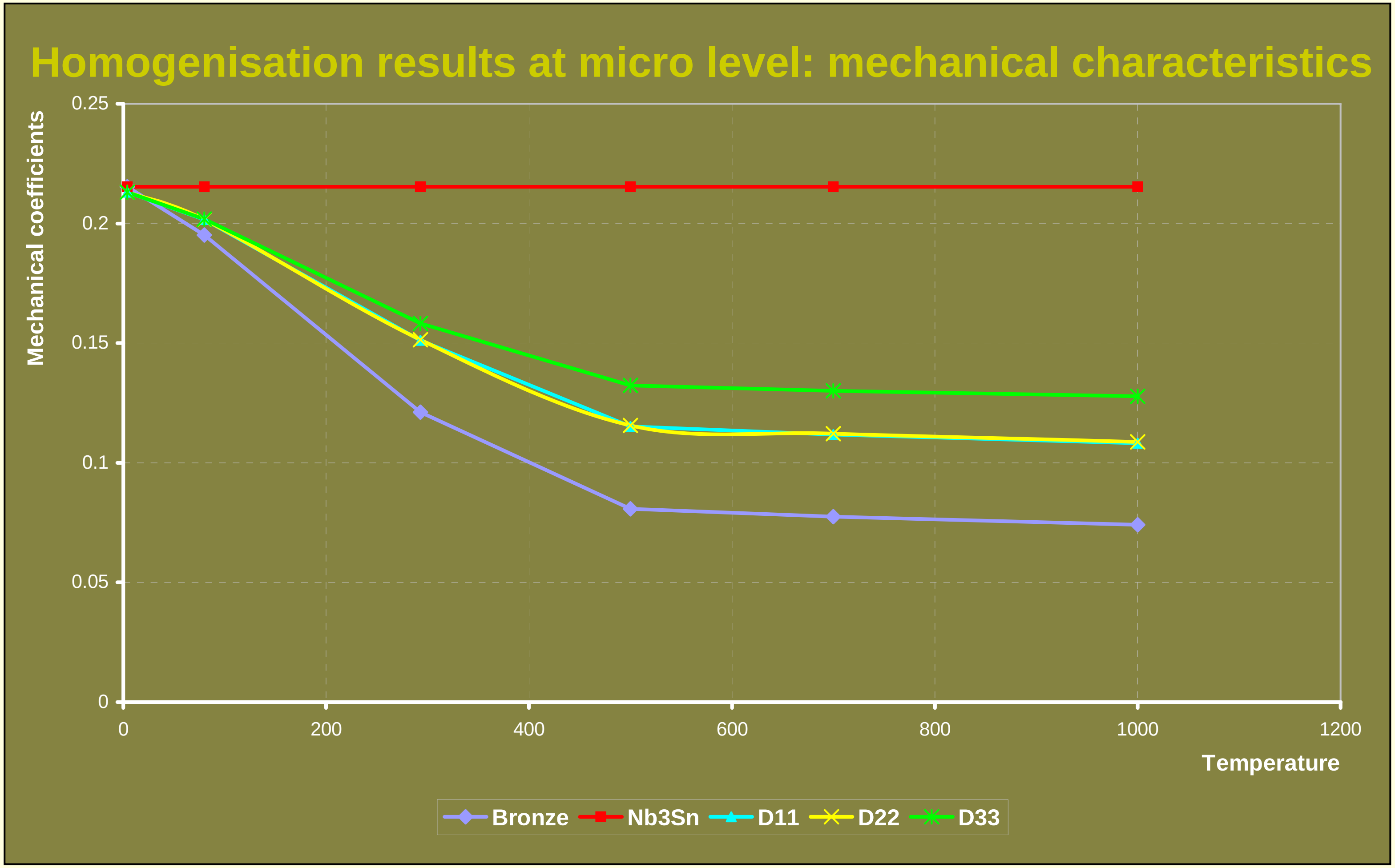

Elasticity tensor coefficients [N/micron^2]

A three-scale model for EAS strands

University of Padua

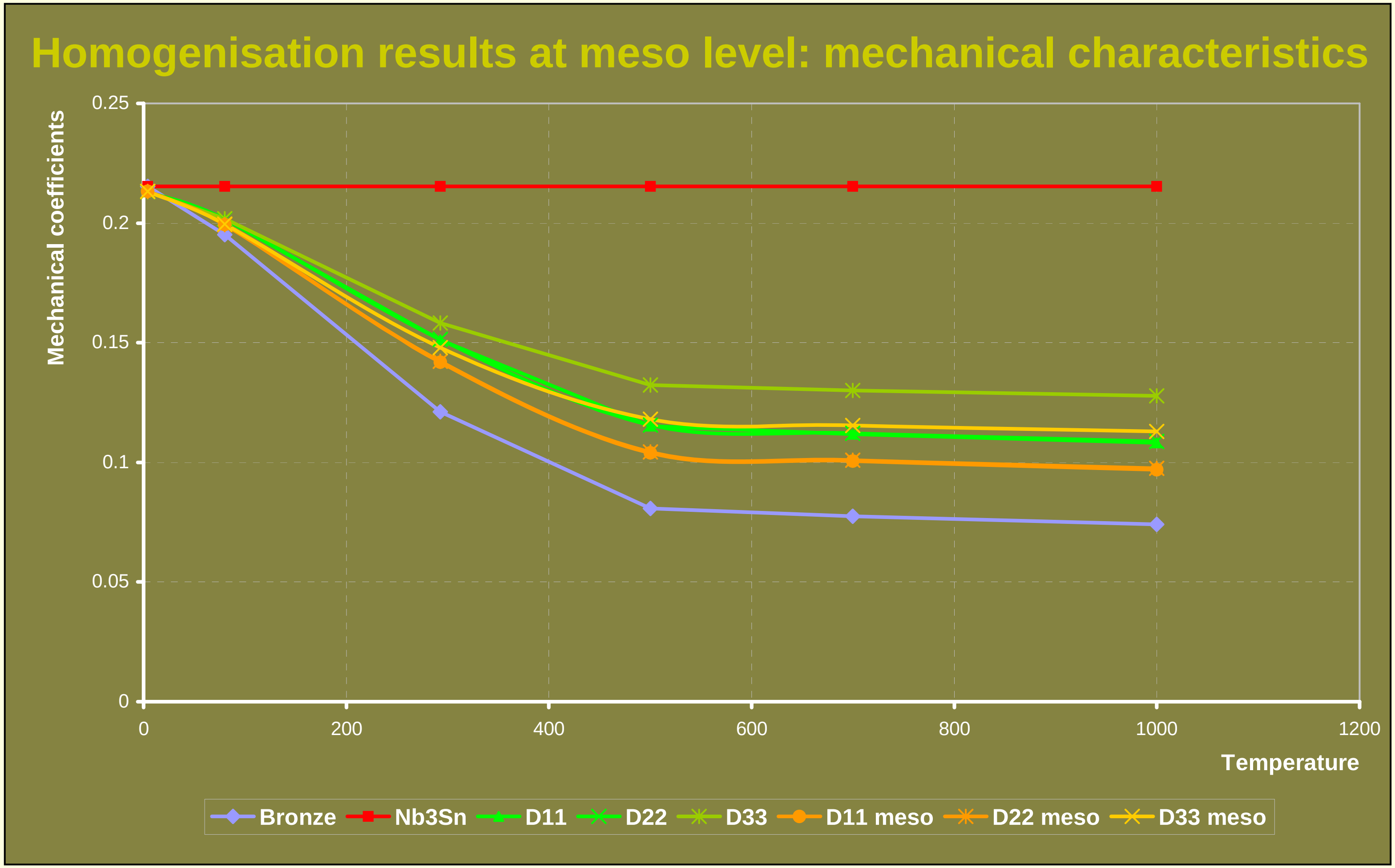

Elasticity tensor coefficients [N/micron^2]

Single strand: strain due to cool down

University of Padua

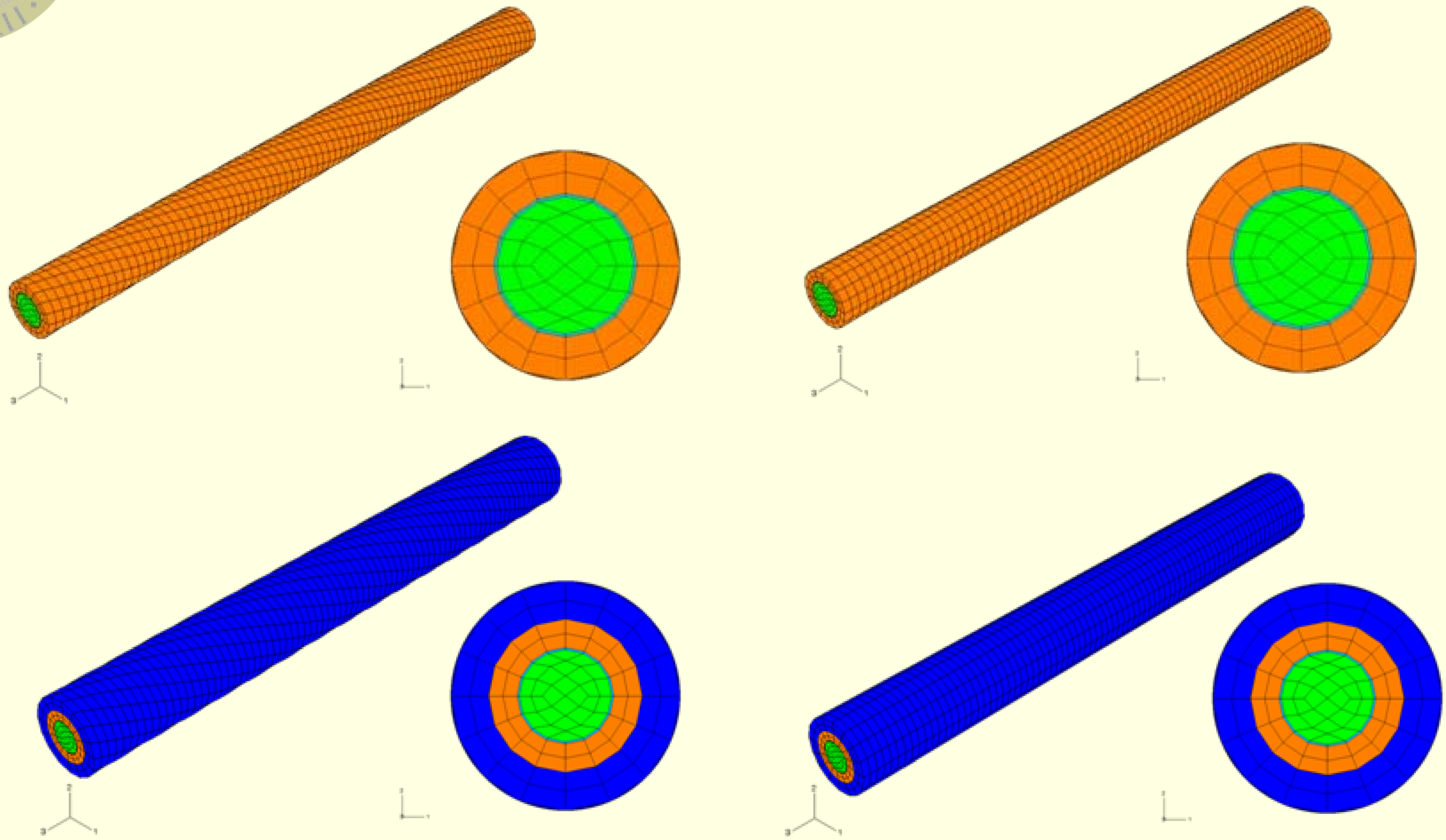

EAS strand models: twisted, untwisted, jacket+twisted, jacket+untwisted

Single strand: comparison with experimental results

Thermal strain ε_{th}	Nb3Sn (Unsmearing)	Bronze (Unsmearing)	Copper	Steel
Twisted no Jacket	-0.0068	-0.0133	-0.0152	-
Unwisted no Jacket	-0.0068	-0.0133	-0.0152	-
Twisted with Jacket	-0.0068	-0.0133	-0.0152	-0.0152
Untwisted with Jacket	-0.0068	-0.0133	-0.0152	-0.0152

Very good agreement with literature values

Mechanical strain ε_{mech}	Nb3Sn (Unsmearing)	Bronze (Unsmearing)	Copper	Steel
Twisted no Jacket	-0.0028	0.0036	0.0055	-
Unwisted no Jacket	-0.00275	0.0037	0.0057	-
Twisted with Jacket	-0.0080	-0.0015	0.0004	0.0004
Untwisted with Jacket	-0.0079	-0.0013	0.0006	0.0006

Very good agreement with FZK experimental results

Single strand: comparison with experimental results

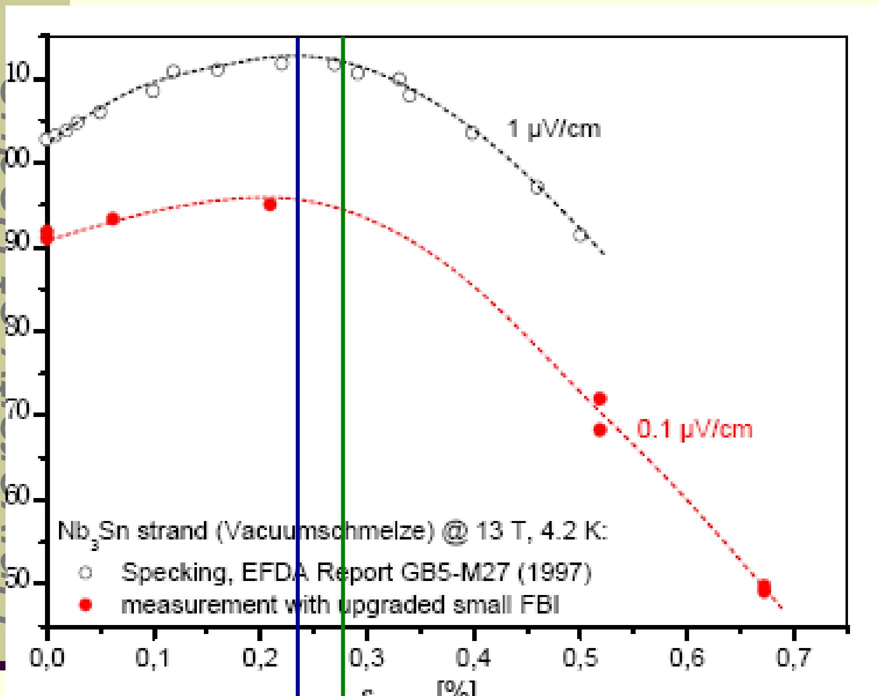

Measured Computed

EAS (Vacuumschmelze) strand
without jacket

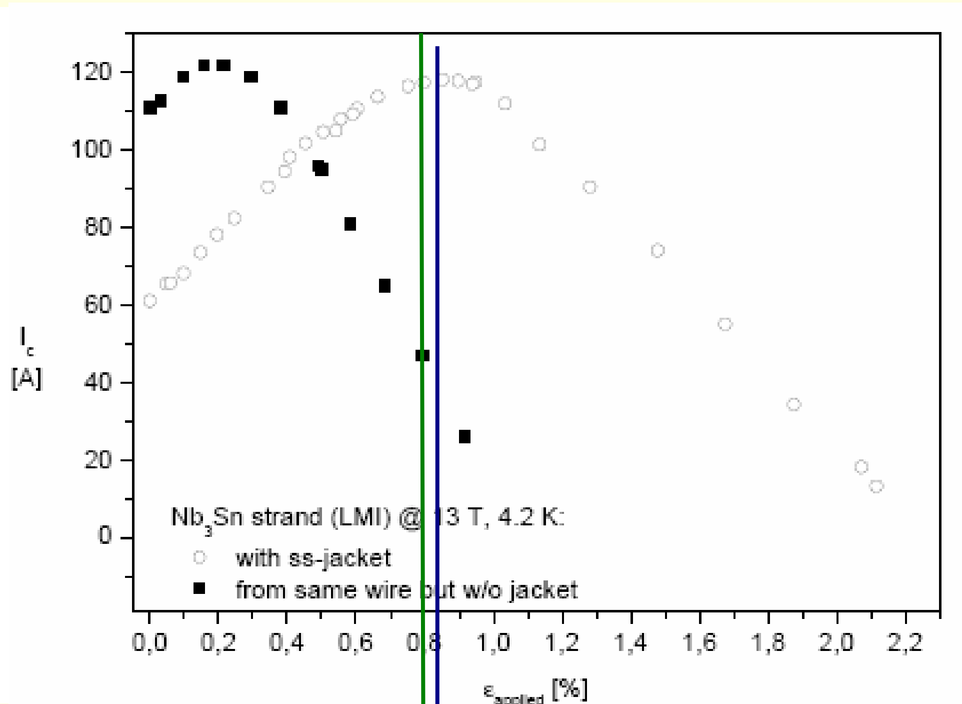

Computed Measured

LMI (Europa Metalli) strand
with jacket

Hierarchical beam model - numerical results

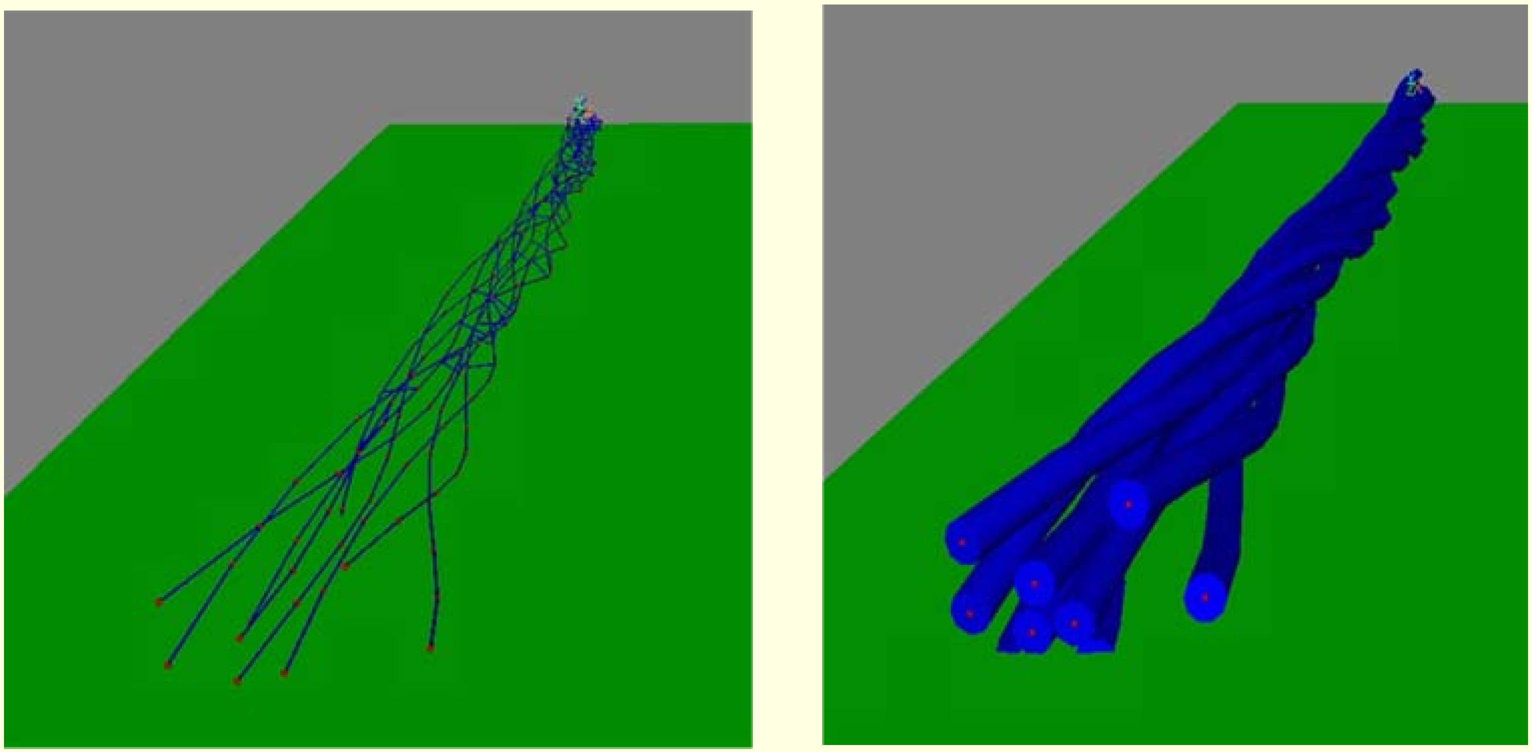

View of a 3x3 bundle of strands in their final configuration

Hierarchical beam model - numerical results

University of Padua

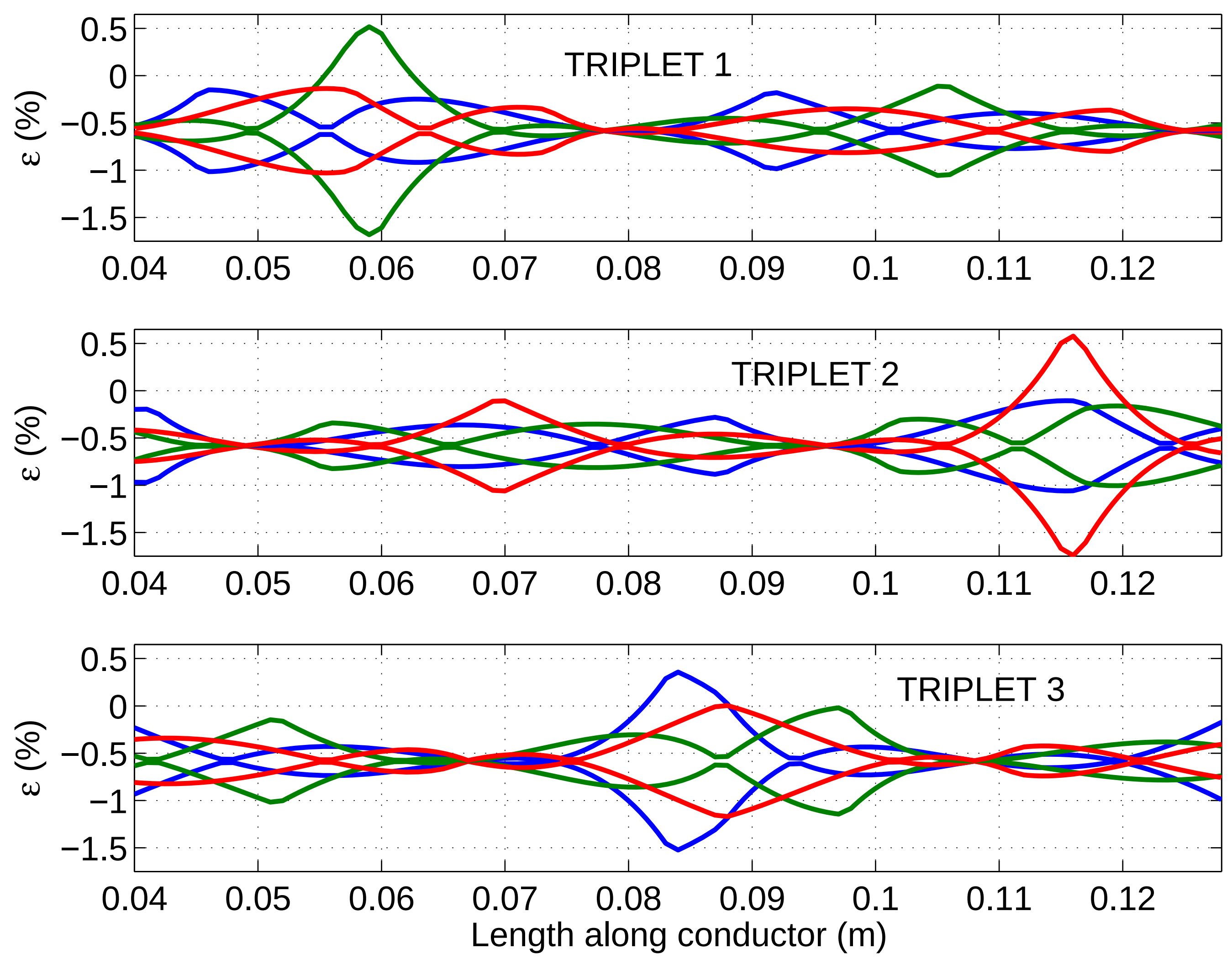

Red: strand 1, min and max values

Blue: strand 2, min and max values

Green: strand 3, min and max values

Comparison with experimental results

$$V_{comp} = \int \langle E \rangle(x)\, dx$$

Issue** = relation between ∫<E>(x) dx and **measured** V between voltage taps **on jacket

<u>strand</u> index in the same (B, T, ε) conditions

$$\langle E \rangle(x) = E_c \sum_{k=1}^{n_{strand}} \frac{1}{n_{strand}} \left(\frac{(I_{sc}/A_{sc})^{(k)}}{\frac{2}{\pi\varepsilon_B^2}\int_{-\varepsilon_B}^{+\varepsilon_B} \sqrt{\varepsilon_B^2-\lambda^2}\, j_c[B^{(k)}(x), T^{(k)}(x), \varepsilon_{th+op}{}^{(k)}(x)+\lambda]\, d\lambda} \right)^{n^{(k)}(j_c(B,T,\varepsilon}$$

discrete sum over all strand contributions

Accounting for different contributions [Ekin, 1981]:

$\varepsilon_{th} + \varepsilon_{bend}(y,z)$

Low inter-filament transverse resistivity limit is assumed [A. Nijhuis, 2006]

Results (Ib)

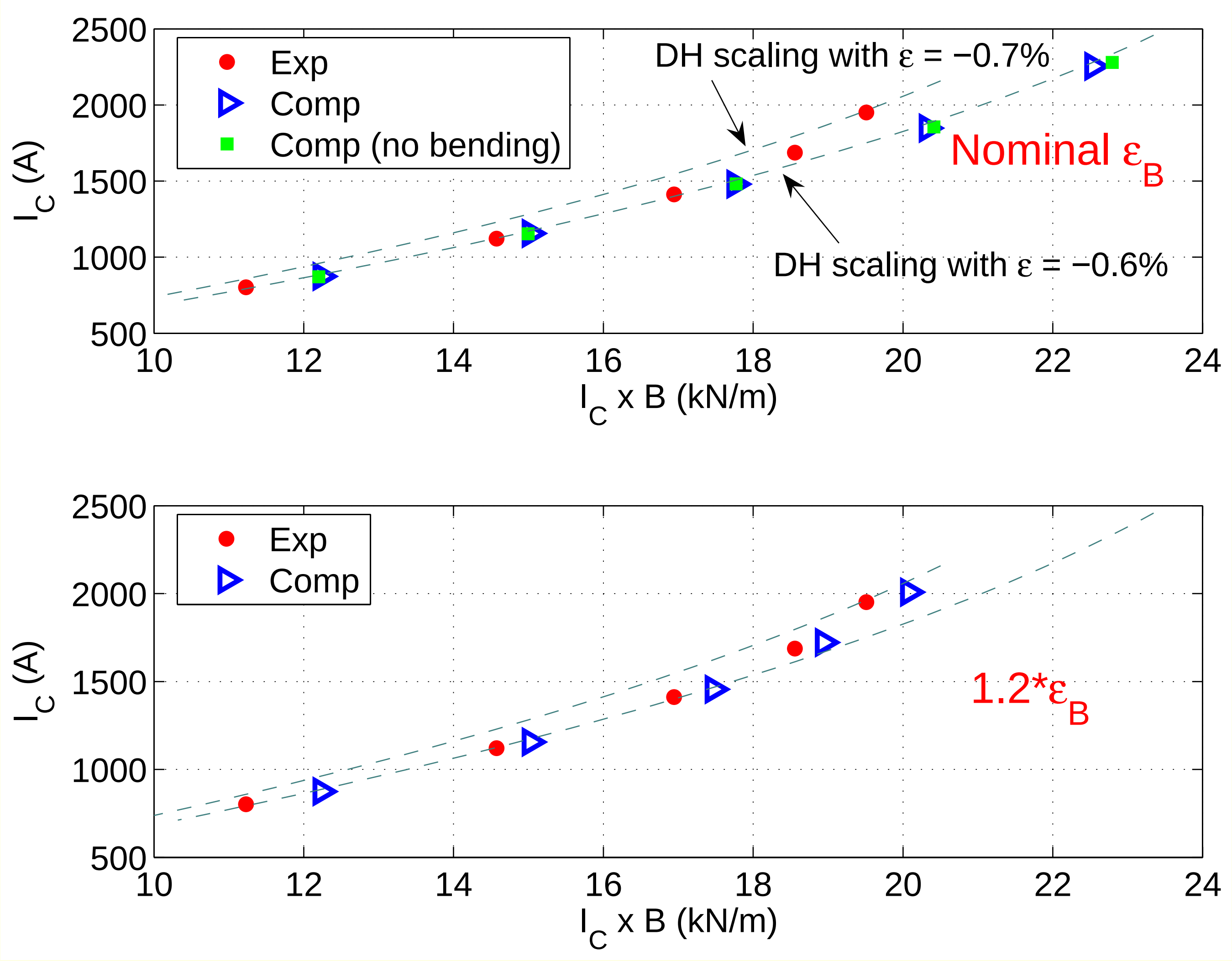

University of Padua

Fire in tunnels: two examples

St.Gotthard fire

Tauern fire

- Hazards for human beings
- Economic difficulties
- Huge repair costs

Physical Model:
Phases of moisture & inner structure of concrete porosity

University of Padua

Critical temperature & Critical point

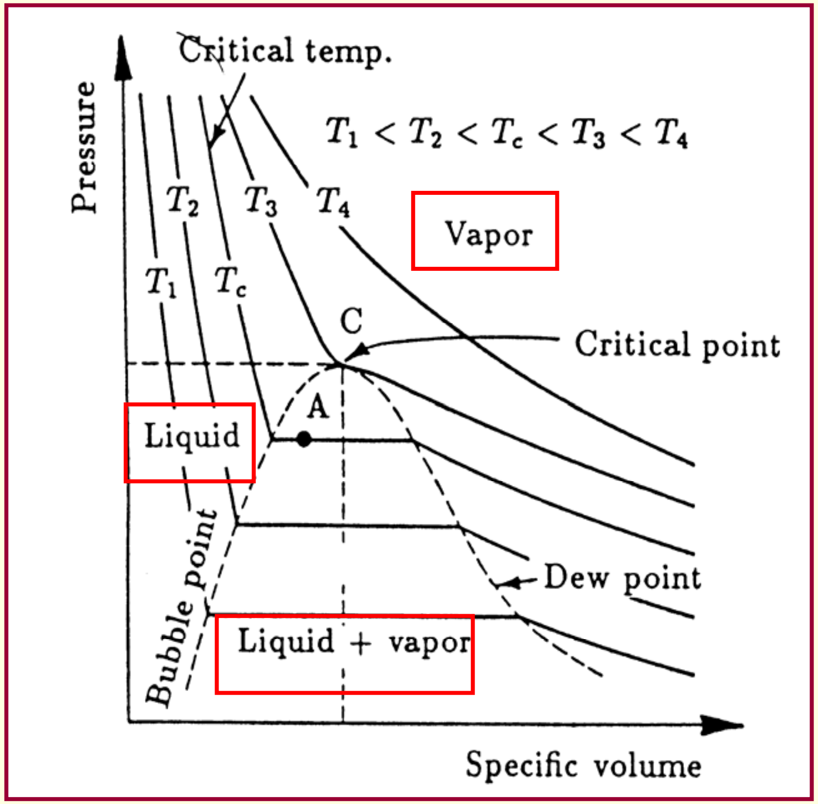

Scanning Electron Microscopy

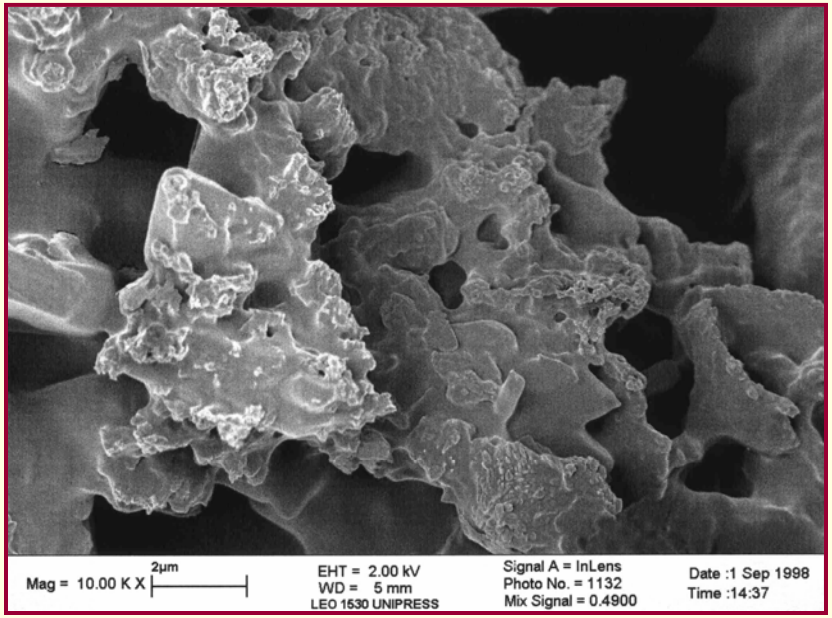

10 000 x

MATHEMATICAL MODEL FOR CONCRETE:
Macroscopic balance equations

University of Padua

Dry air mass balance equation

$$-n\frac{D^sS_w}{Dt}-\beta_s(1-n)S_g\frac{D^sT}{Dt}+S_g\,div\,\mathbf{v}^s+\frac{S_g n}{\rho^{ga}}\frac{D^s\rho^{ga}}{Dt}+\frac{1}{\rho^{ga}}div\,\mathbf{J}_g^{ga}+\frac{1}{\rho^{ga}}div\left(nS_g\rho^{ga}\mathbf{v}^{gs}\right)$$

$$-\frac{(1-n)S_g}{\rho^s}\frac{\partial\rho^s}{\partial\Gamma_{dehydr}}\frac{D^s\Gamma_{dehydr}}{Dt}=\frac{\dot m_{dehydr}}{\rho^s}S_g$$

Water species (liquid+vapour) mass balance equation

$$n\left(\rho^w-\rho^{gw}\right)\frac{D^sS_w}{Dt}+\left(\rho^wS_w+\rho^{gw}S_g\right)\alpha\,div\,\mathbf{v}^s-\beta_{swg}^*\frac{D^sT}{Dt}+S_g n\frac{D^s\rho^{gw}}{Dt}+div\,\mathbf{J}_g^{gw}$$

$$+div\left(nS_w\rho^w\mathbf{v}^{ws}\right)+div\left(nS_g\rho^{gw}\mathbf{v}^{gs}\right)-\left(\rho^wS_w+\rho^{gw}S_g\right)\frac{(1-n)}{\rho^s}\frac{\partial\rho^s}{\partial\Gamma_{dehydr}}\frac{D^s\Gamma_{dehydr}}{Dt}$$

$$=\frac{\dot m_{dehydr}}{\rho^s}\left(\rho^wS_w+\rho^{gw}S_g-\rho^s\right)$$

where: $\beta_{swg}^*=\beta_s(1-n)\left(S_g\rho^{gw}+\rho^wS_w\right)+n\beta_w\rho^wS_w$

MATHEMATICAL MODEL FOR CONCRETE: *Macroscopic balance equations*

Energy balance equation (for whole system)

$$\left(\rho C_p\right)_{eff}\frac{\partial T}{\partial t}+\left(\rho_w C_p^w \mathbf{v}^w+\rho_g C_p^g \mathbf{v}^g\right)\cdot grad\,T-div\left(\chi_{eff}\,grad\,T\right)=-\dot{m}_{vap}\Delta H_{vap}+\dot{m}_{dehydr}\Delta H_{dehydr}$$

Linear momentum balance equation

(for the multiphase system)

$$div\,\boldsymbol{\sigma}+\rho\,\mathbf{g}=0$$

where: $\rho=\left(1-n\right)\rho^s+n\,S_w\rho^w+n\,S_g\,\rho^g$

Causes of thermal spalling

University of Padua

High pressure of vapour

+

water from dehydration

moisture clog

Spall of concrete

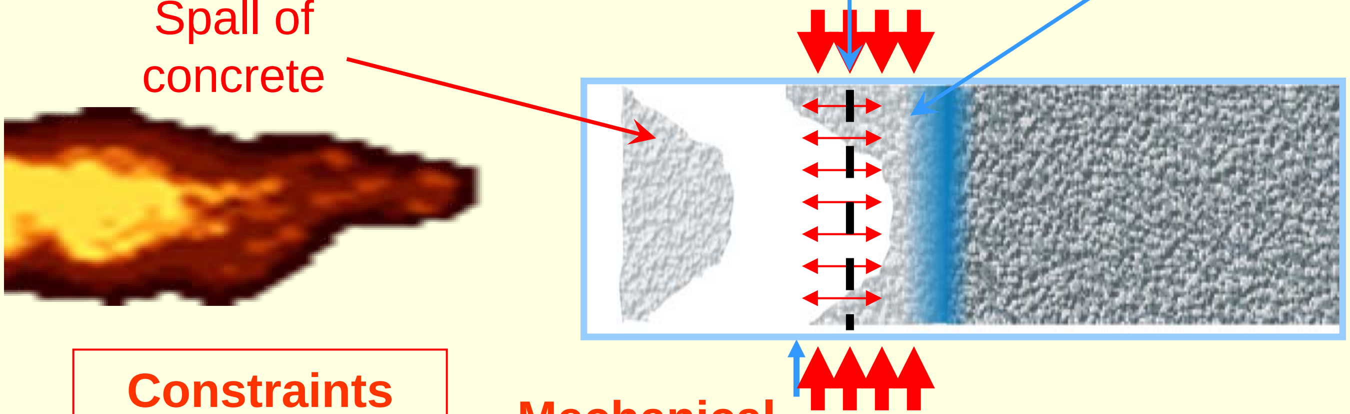

Constraints for thermal dilatation → **Mechanical stresses**

stresses:
aggregate - cem. matrix
+
thermal degradation
+
chemical degradation

Fire tests of HPC elements

Spalling of the C-60 unloaded column

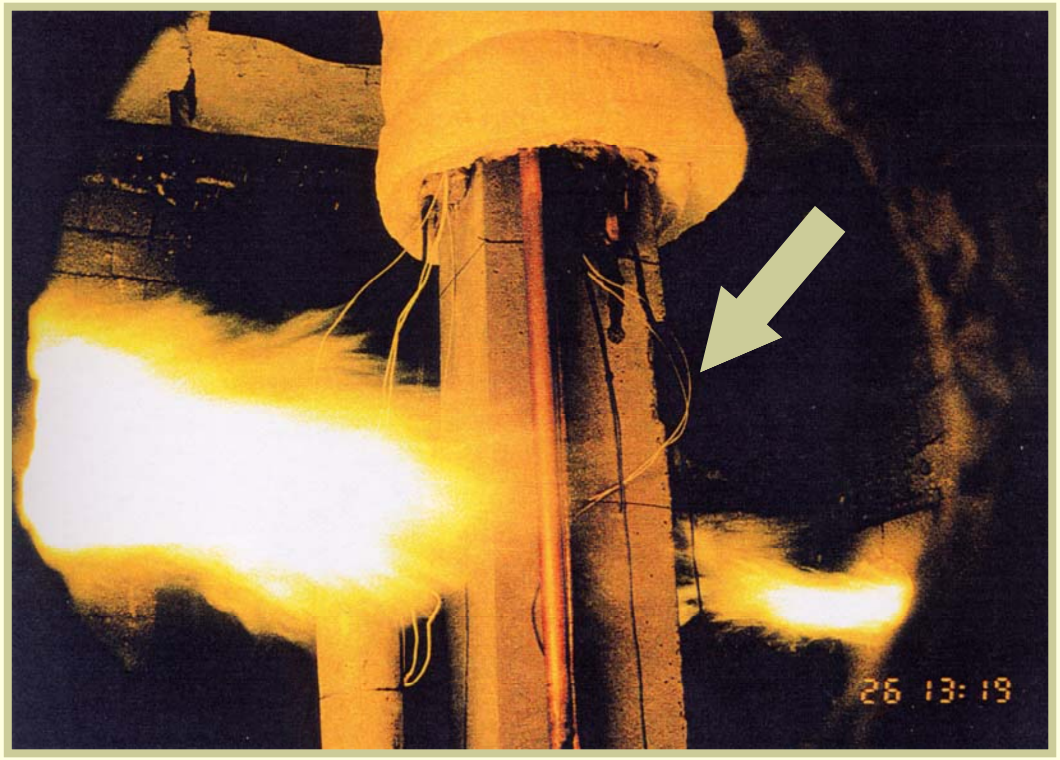

Square column subjected to ISO-Fire

Temperature & relative humidity after 20 min. of fire

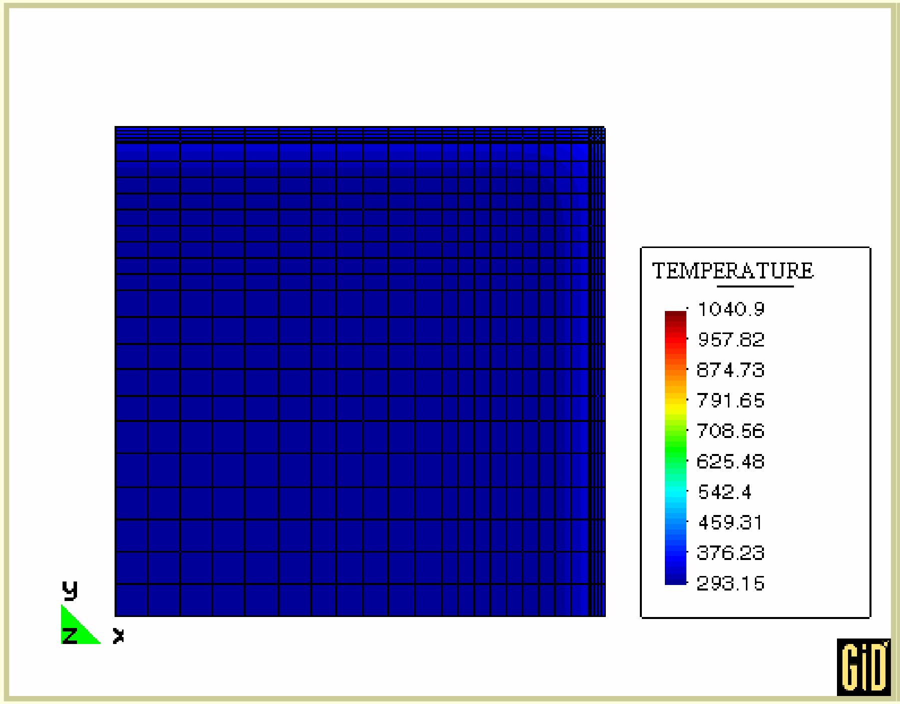

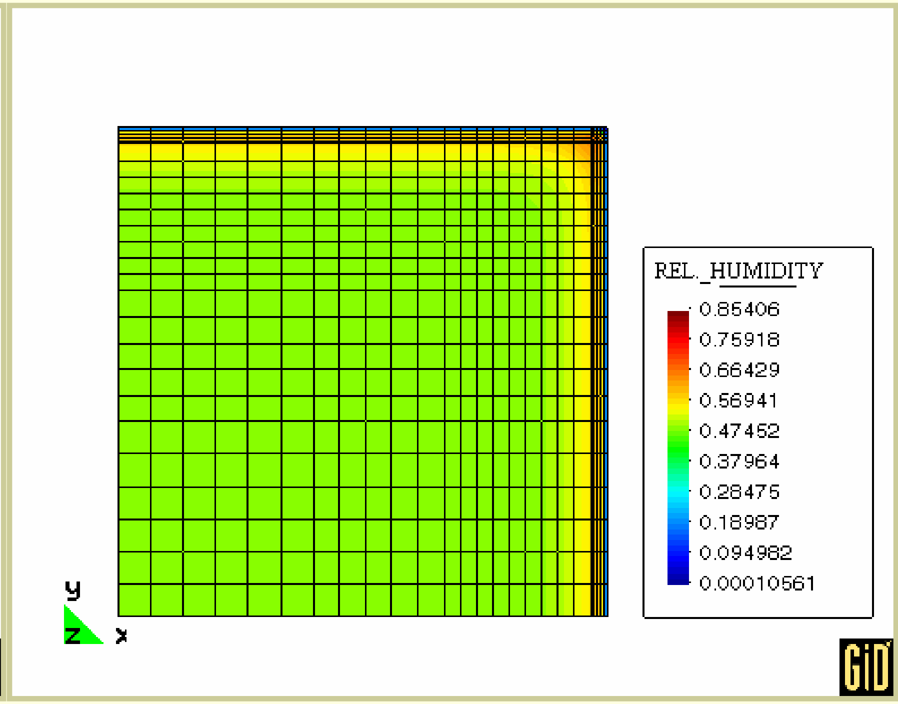

C-60 concrete

Square column subjected to ISO-Fire

Vapour pressure & total damage after 20 min. of fire

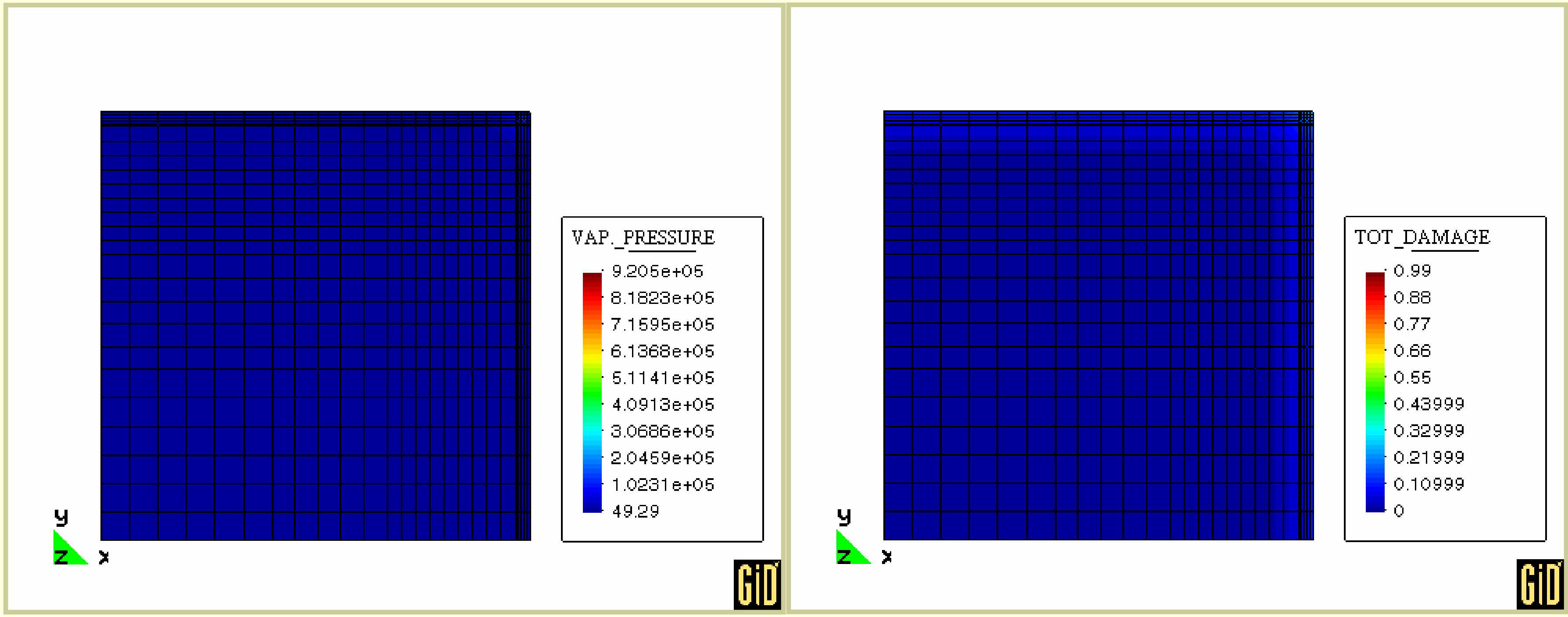

C-60 concrete

Fire in tunnels: two examples

University of Padua

St.Gotthard fire

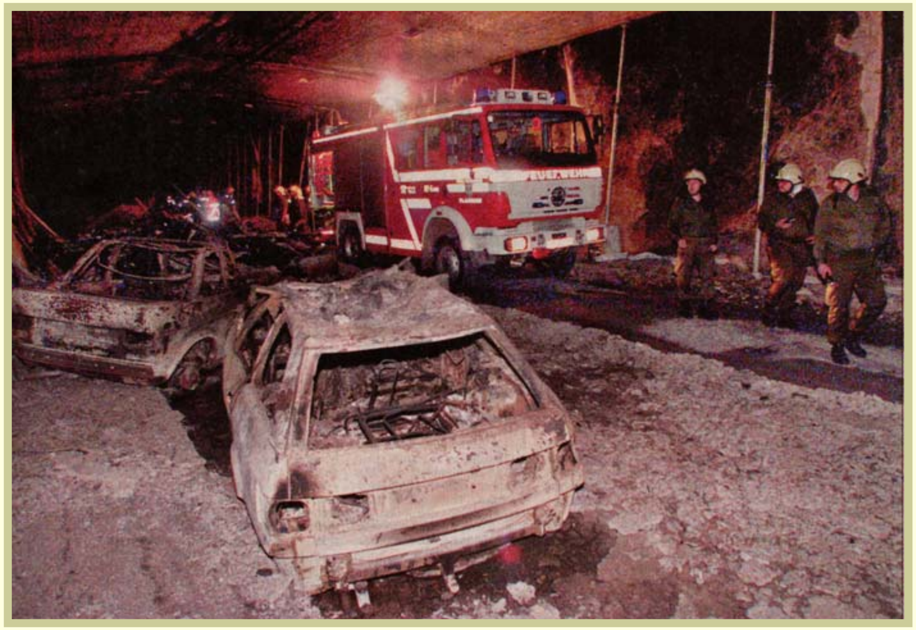

Tauern fire

- Hazards for human beings
- Economic difficulties
- Huge repair costs

Fire in tunnels: phenomena involved

- Heat transfer:
  - Thermal radiation with media participation
  - Presence of smoke, soot, dust particles
  - Conduction through tunnel vault
  - Convection due to the flow movement
  - …
- Combustion processes:
  - Volumetric heat source
  - Eddy break-up
  - …
- Thermo-fluid-dynamics:
  - Computational Fluid Dynamics
  - Turbulent flows
  - Heat generation / sink
  - …
- Structural behaviour of the concrete:
  - Multiphase porous material model
  - High temperature gradients
  - Spalling phenomena

Fire in tunnels: heat balance

Heat transfer

within the fluid

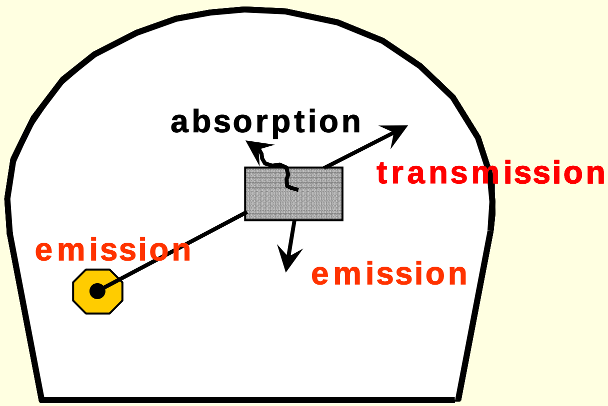

Balance at the tunnel vault

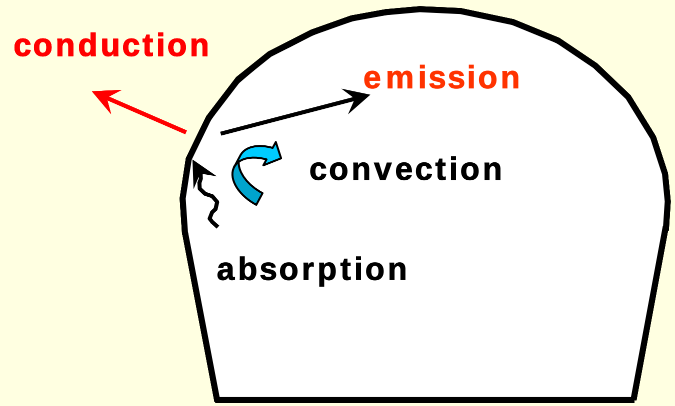

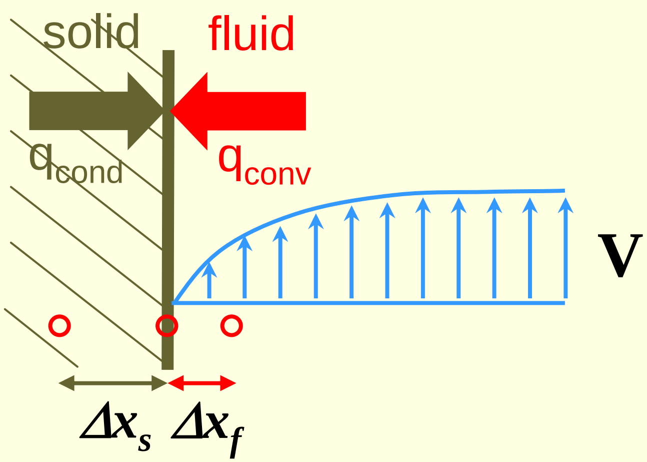

✓Convection coefficient evaluation by means of CFD calculations without radiative fluxes

Thermo-Fluid Dynamics

University of Padua

✓Low Mach number flow
✓Compressible and Newtonian fluid
✓Coupling with the convection-diffusion-reaction equation

Radiative fluxes

$$\begin{cases} \dfrac{D\rho}{Dt} + \rho \nabla \mathbf{u} = S_\rho \\ \rho \dfrac{D\mathbf{u}}{Dt} + \nabla p = \nabla \cdot \left(2\, \mu\, \varepsilon' (\mathbf{u}) \right) + \mathbf{f} \\ \rho\, c_p \dfrac{DT}{Dt} - \beta\, T \dfrac{D\tilde{p}}{Dt} = \nabla \cdot (k \nabla T) + 2\mu\varepsilon' (\mathbf{u}) : \varepsilon' (\mathbf{u}) + \nabla \cdot q_r + S_T \end{cases}$$

- Continuity equation
- Linear momentum balance equation
- Convection-diffusion-reaction equation

Volumetric heat source

Fire in tunnels: heat balance

Radiation with media participation

✓ Heat transfer by radiation affects the temperature distribution both within the fluid and the thermal balance at the wall.

✓ Media participation, e.g. absorption, scattering.

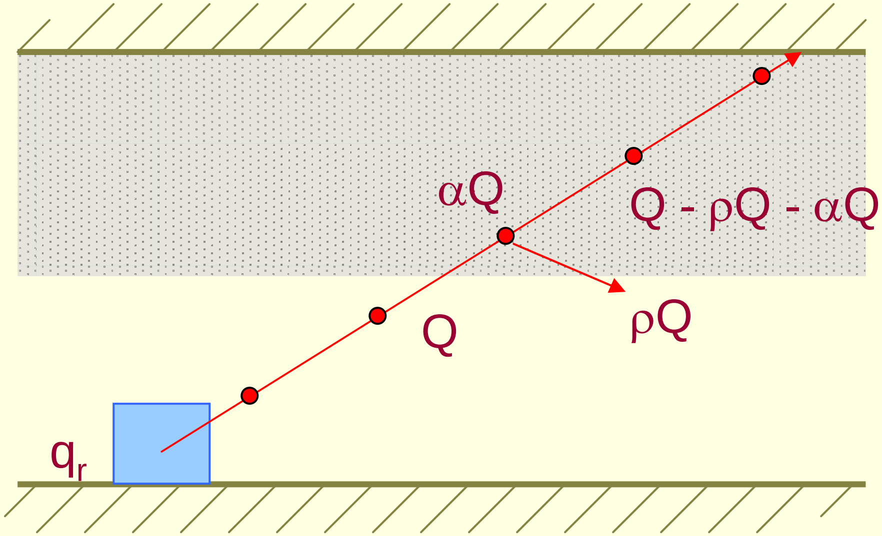

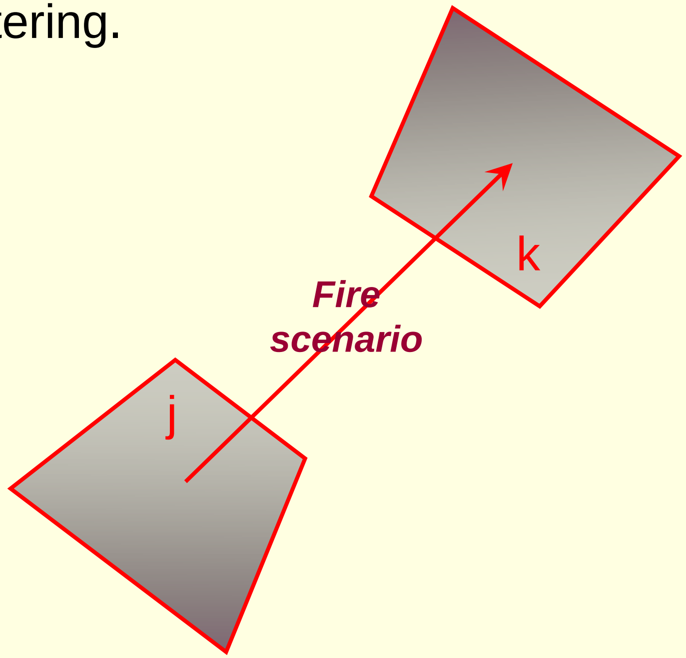

Available codes

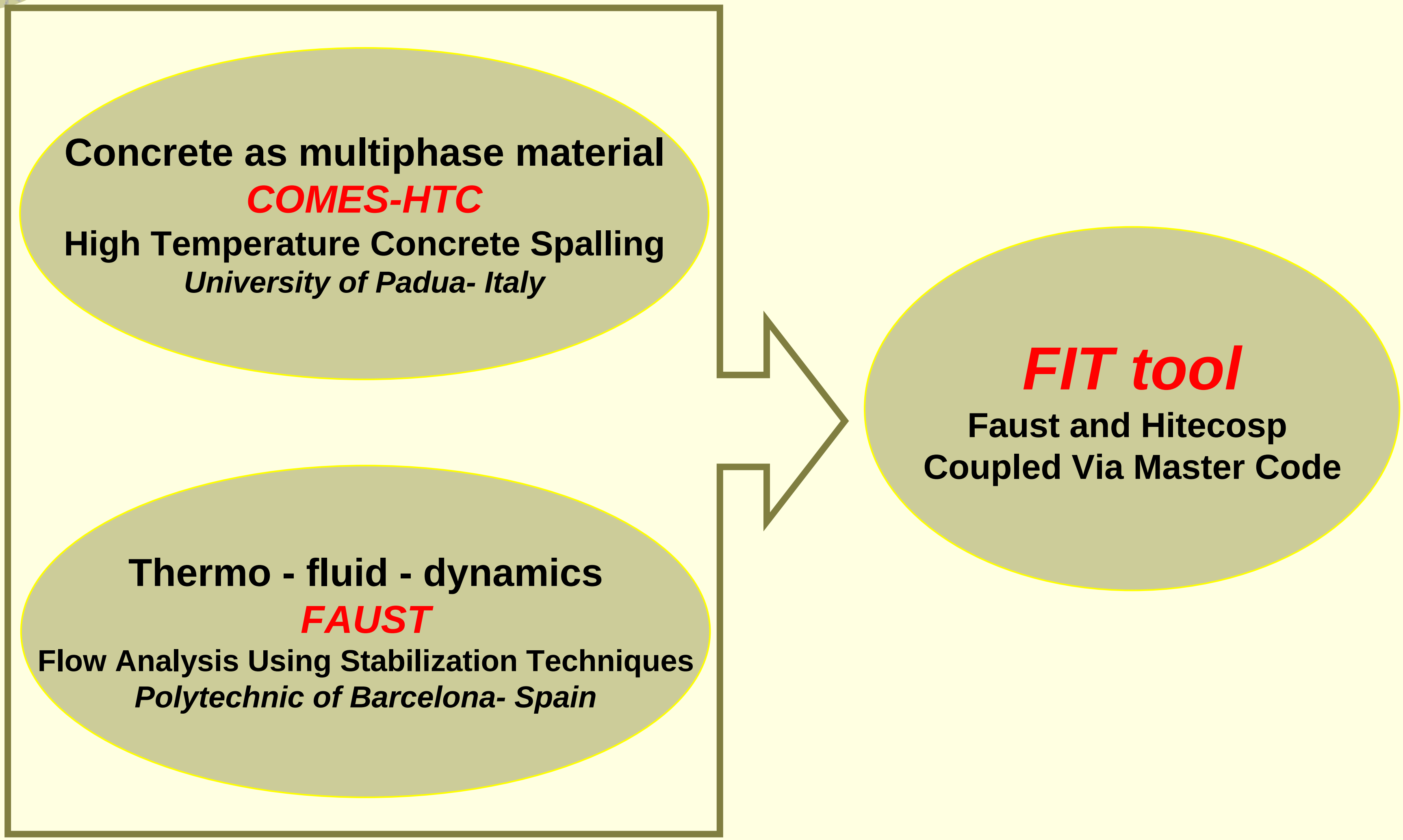

University of Padua

Fire In Tunnel Tool

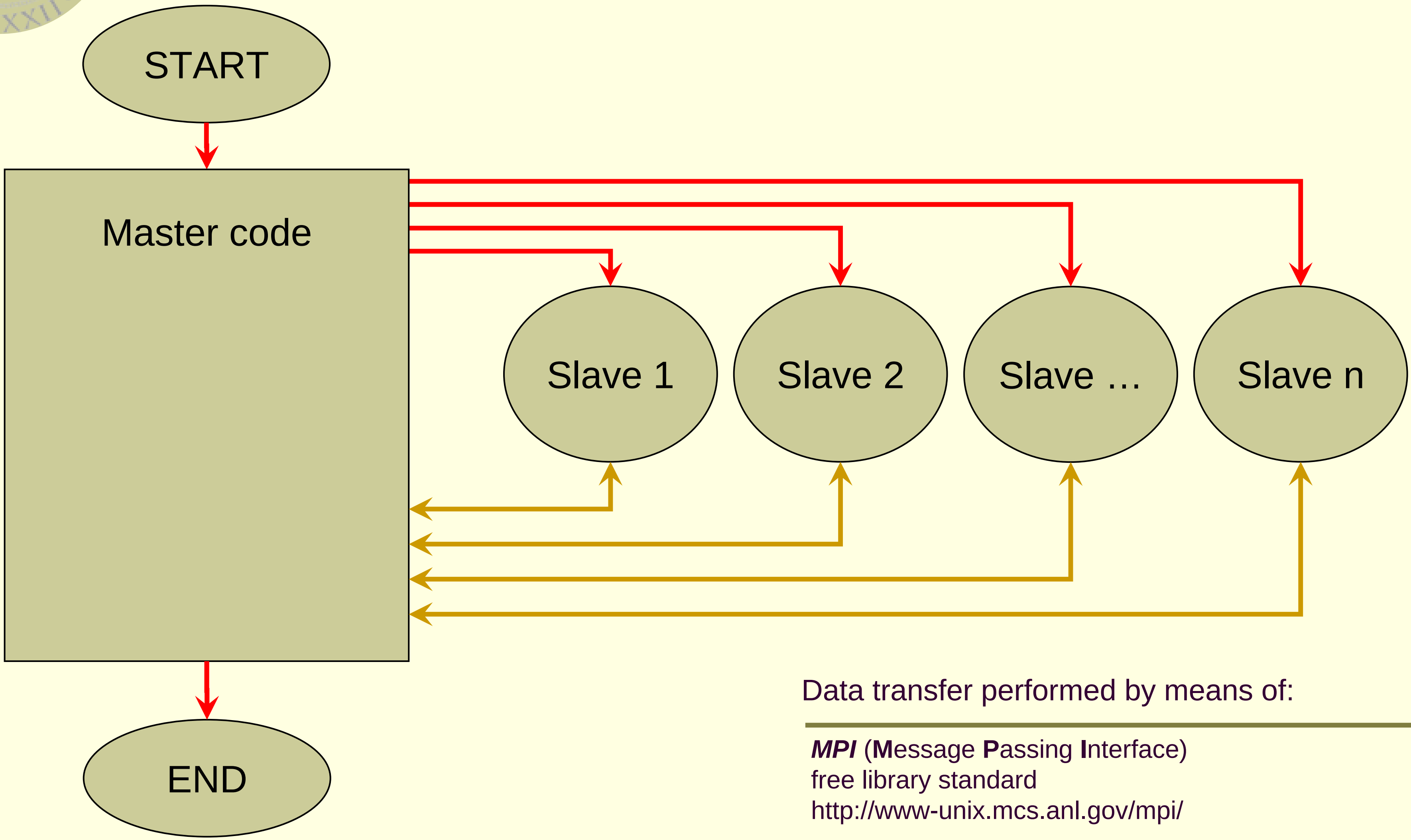

Data transfer performed by means of:

MPI (**M**essage **P**assing **I**nterface)
free library standard
http://www-unix.mcs.anl.gov/mpi/

Level of coupling

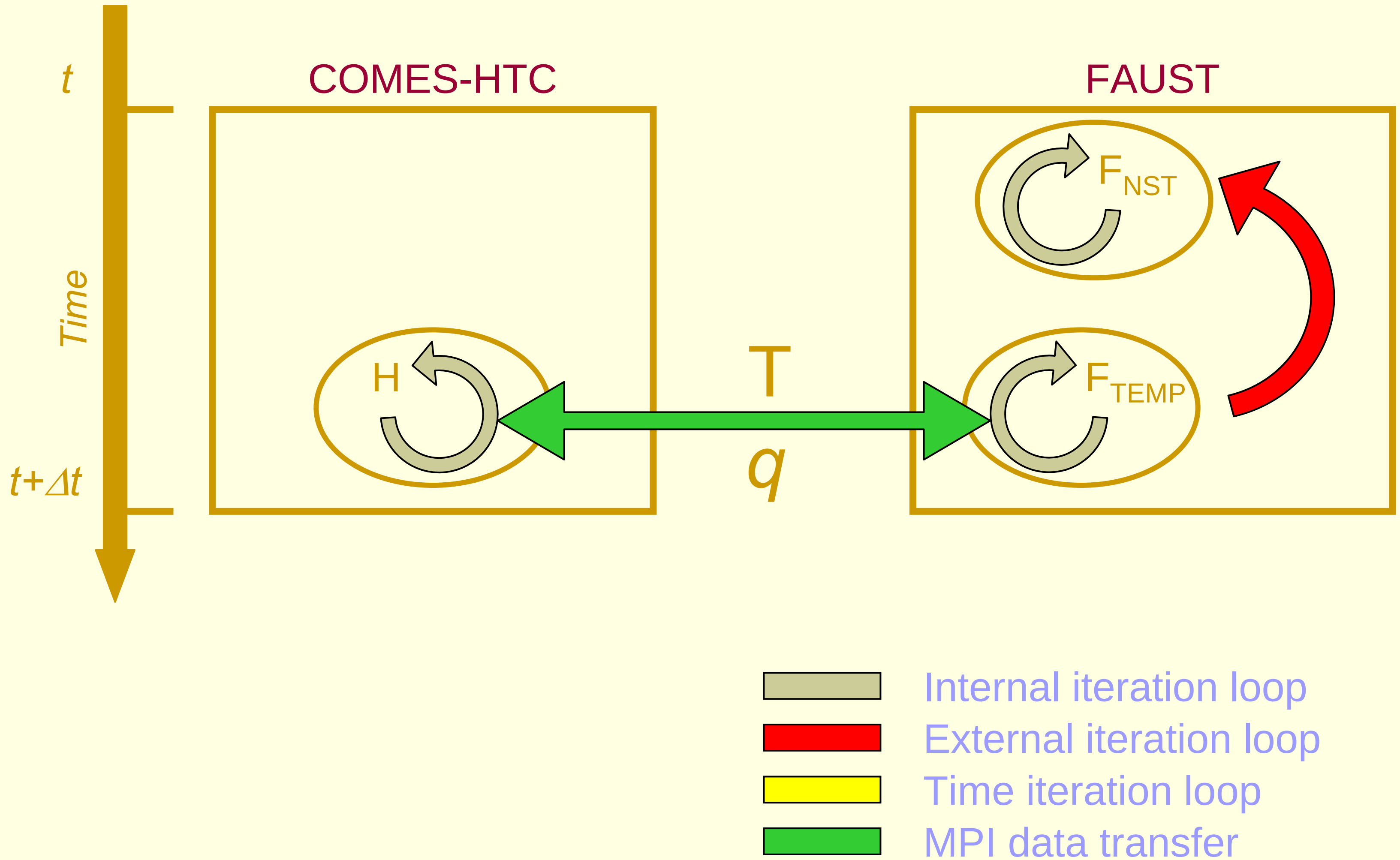

3D to 2D coupling

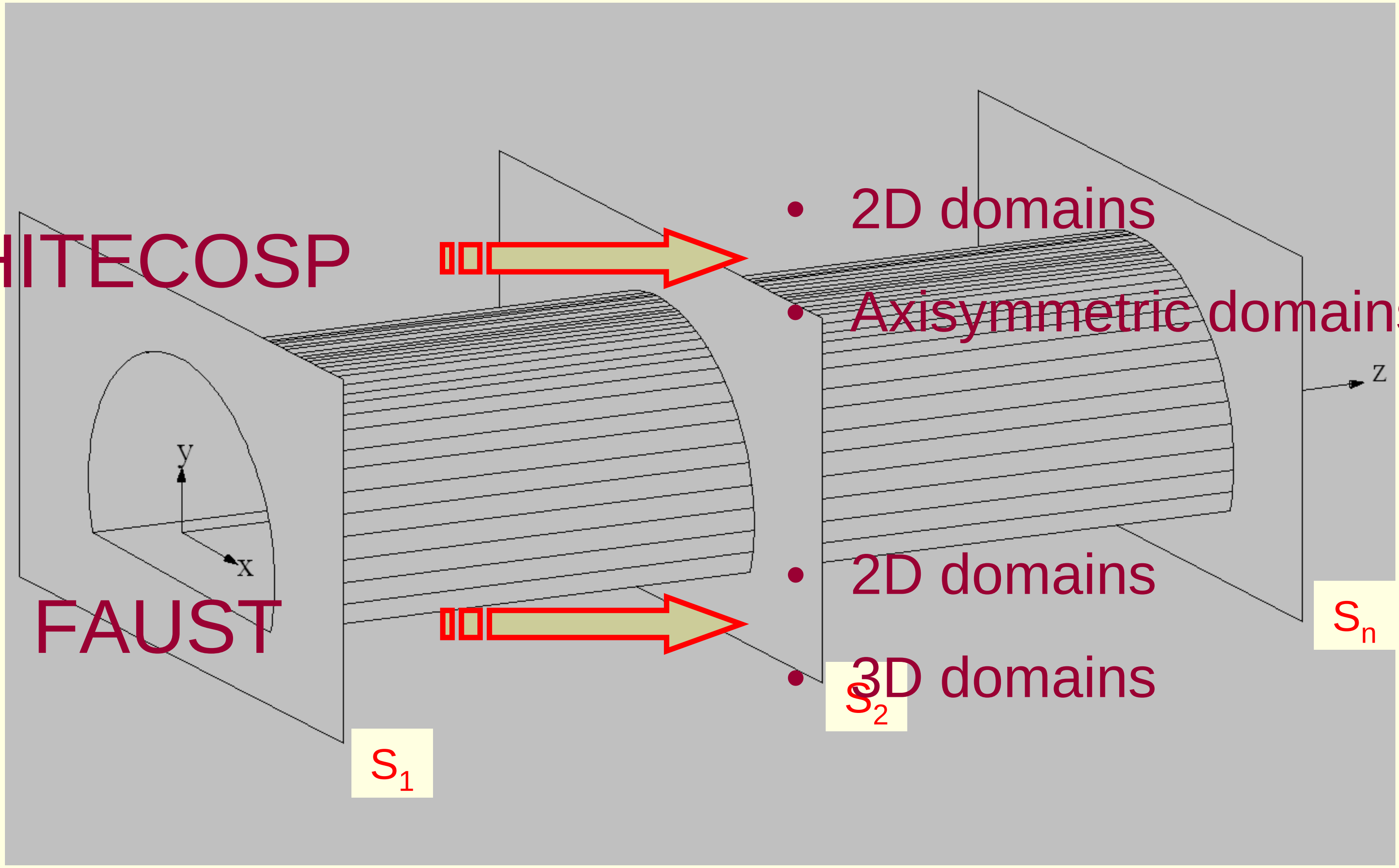

Fluid temperature evolution

University of Padua

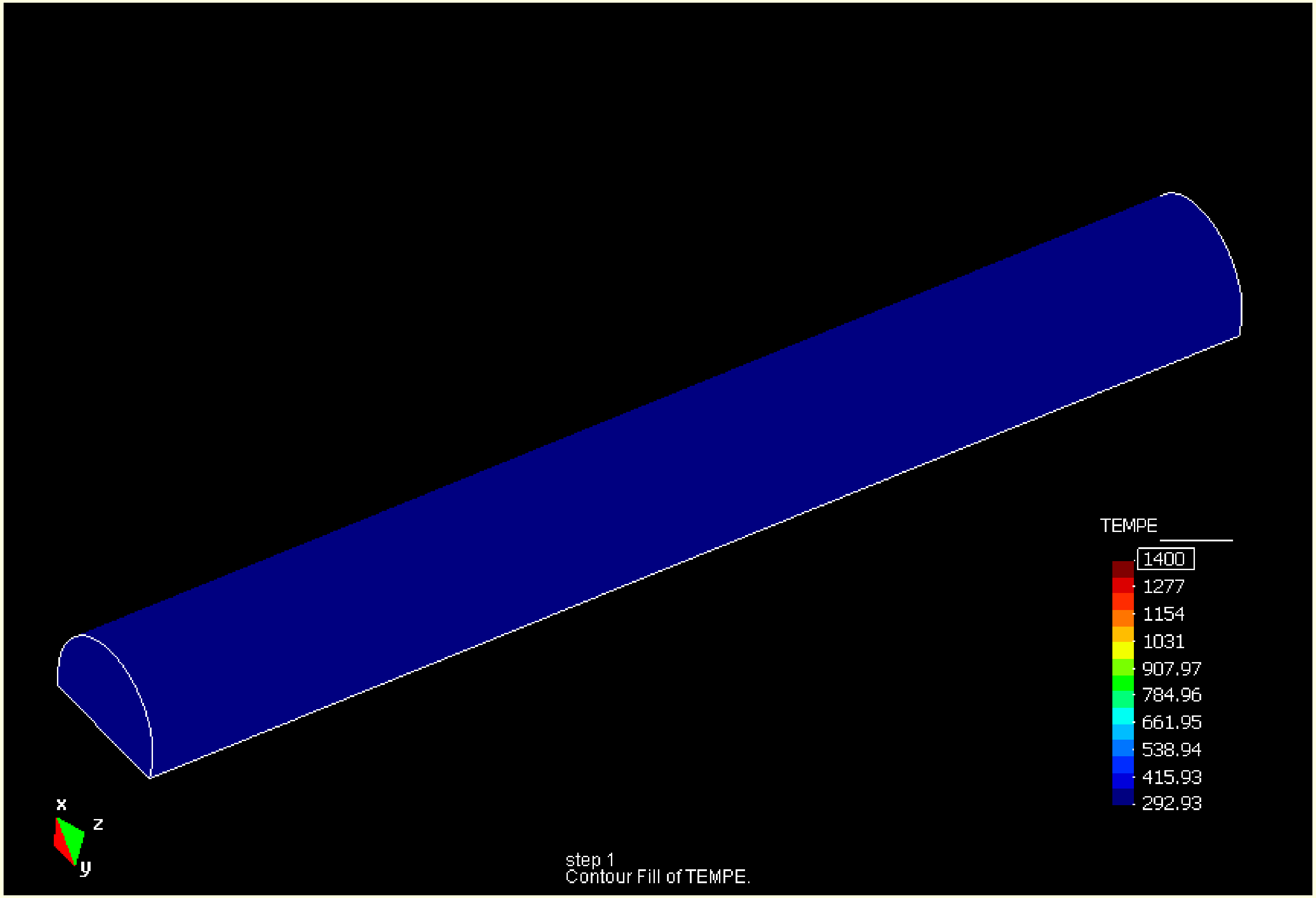

Fluid temperature evolution

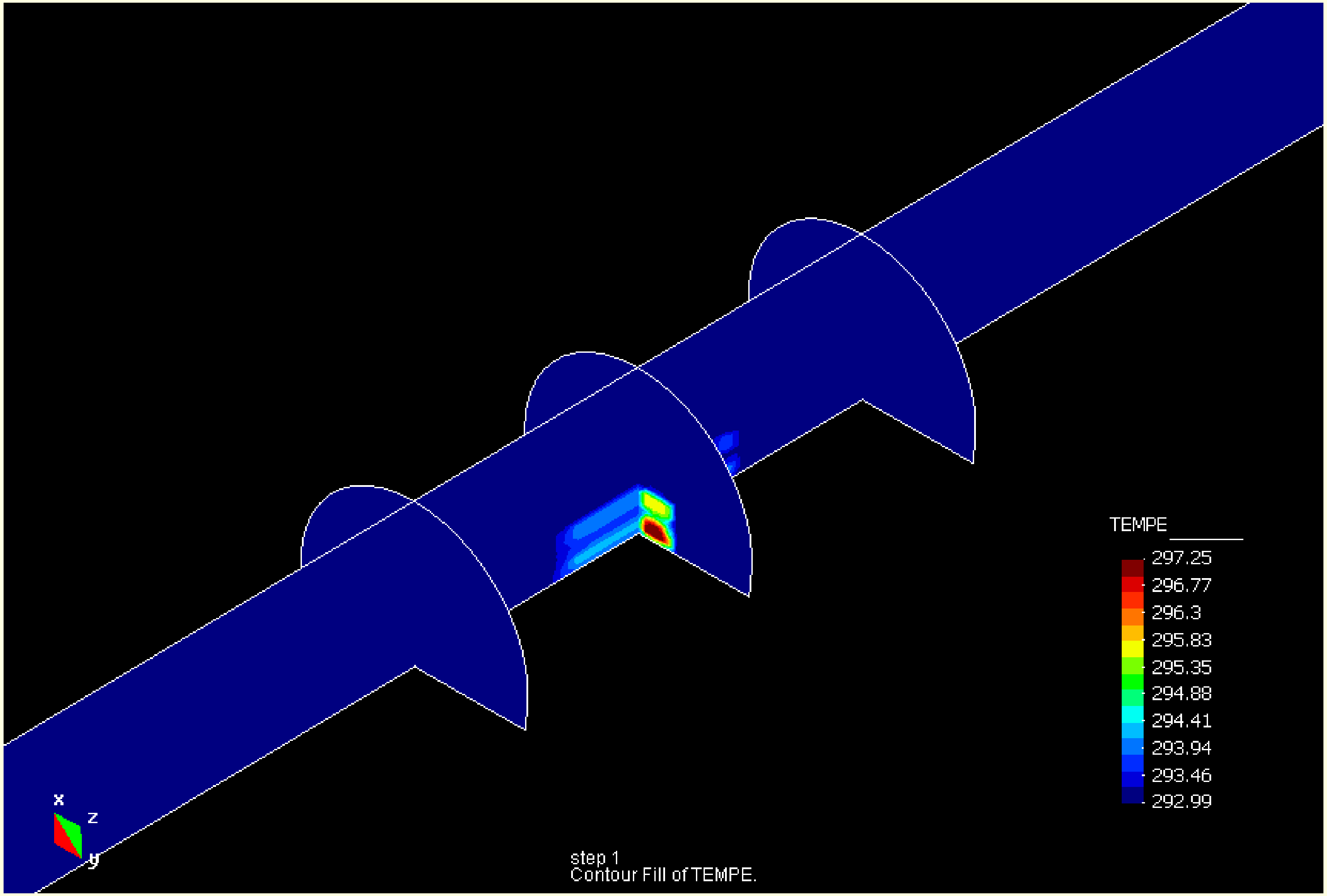

University of Padua

Fluid velocity evolution

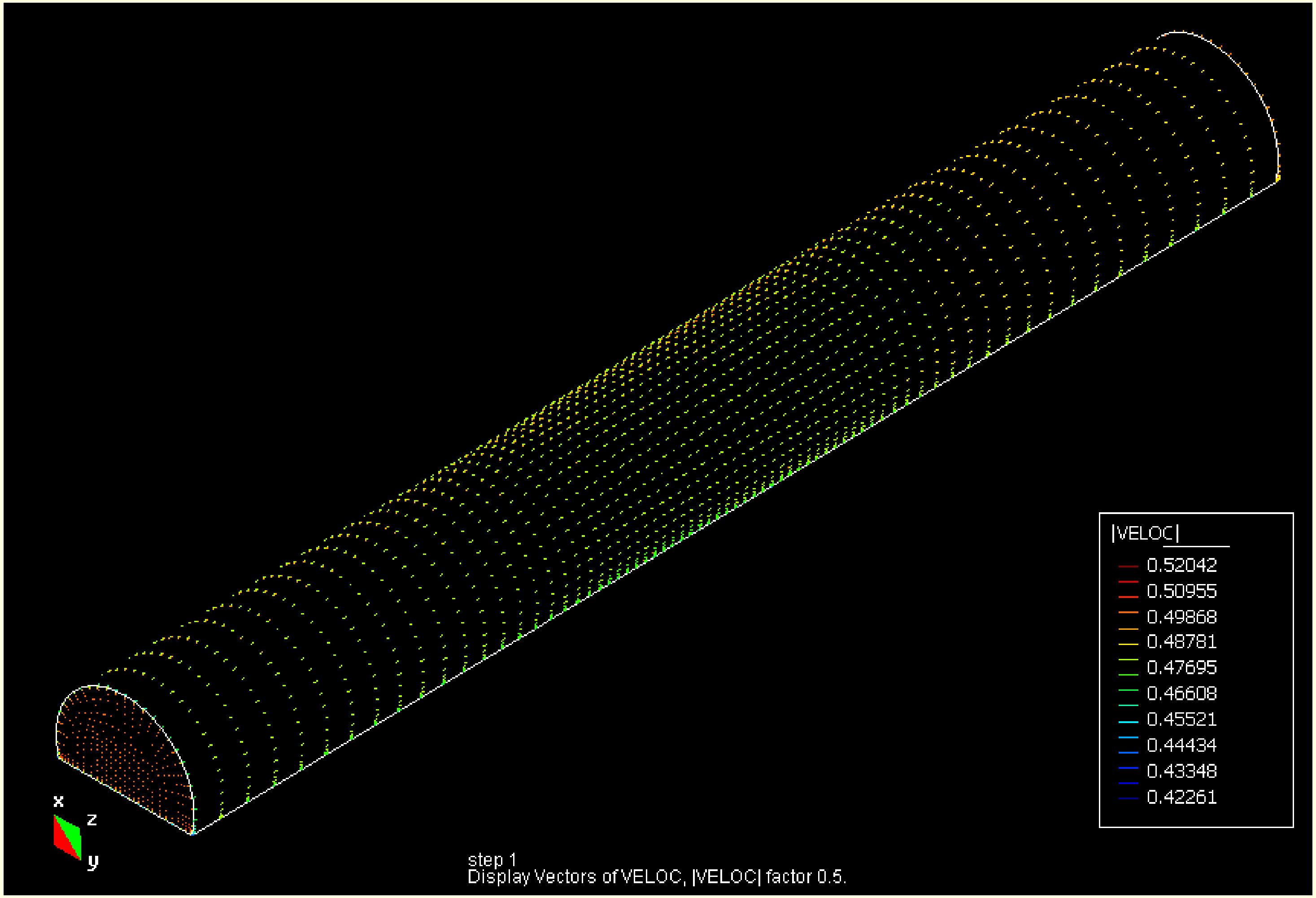

Fluid velocity evolution

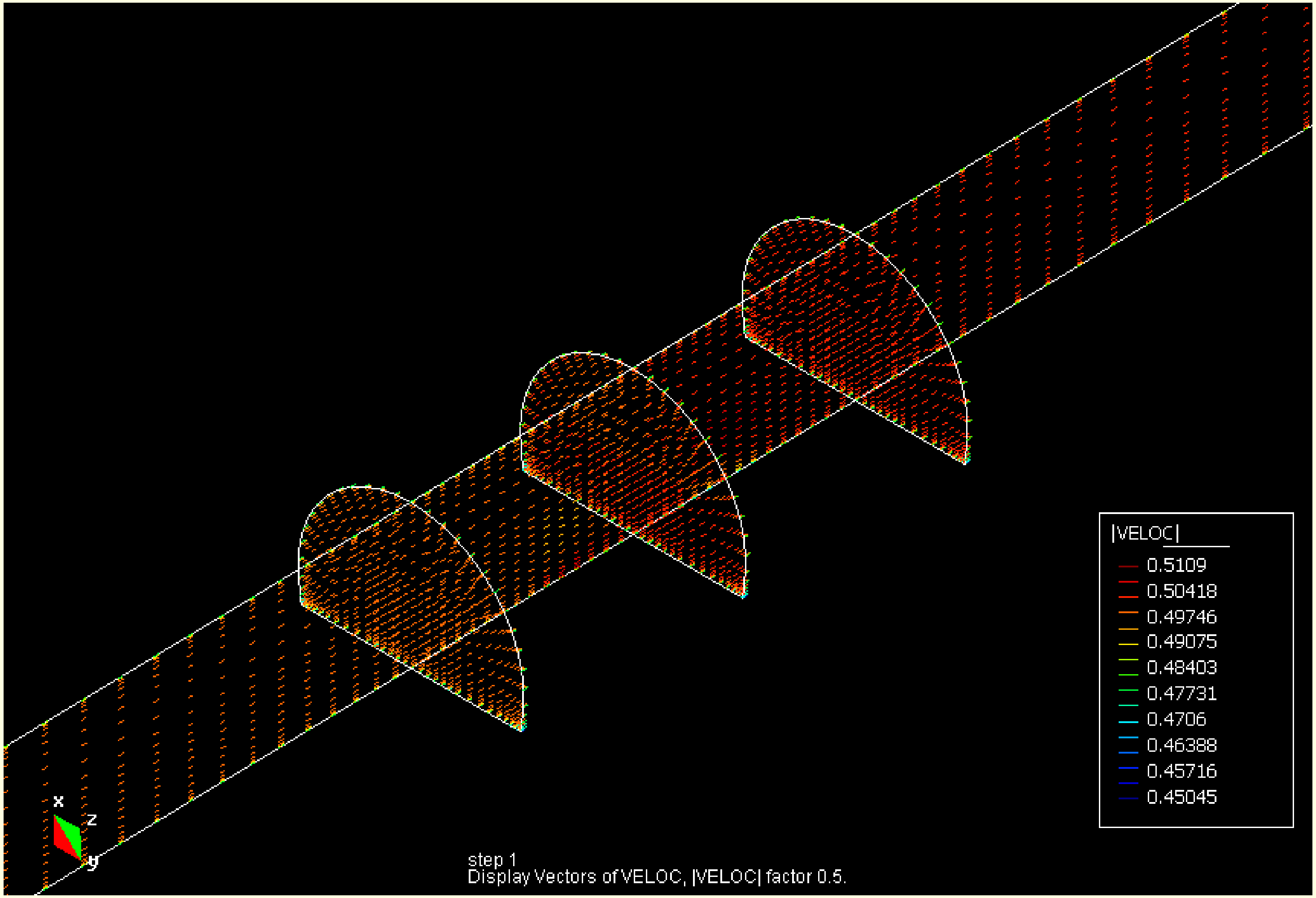

Total damage Distribution

University of Padua

5 min

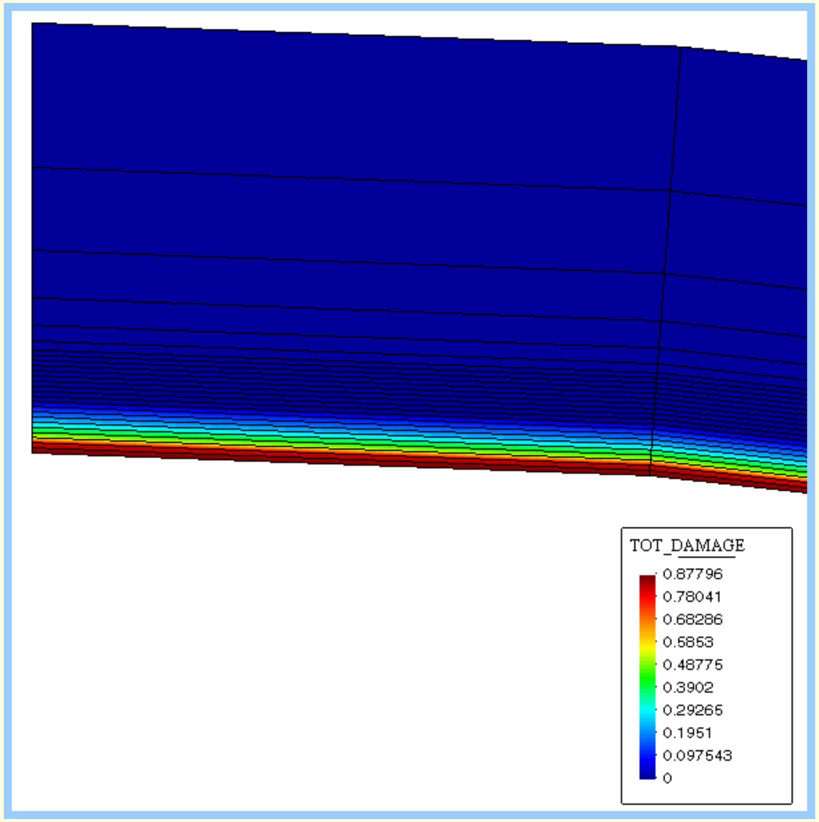

20 min

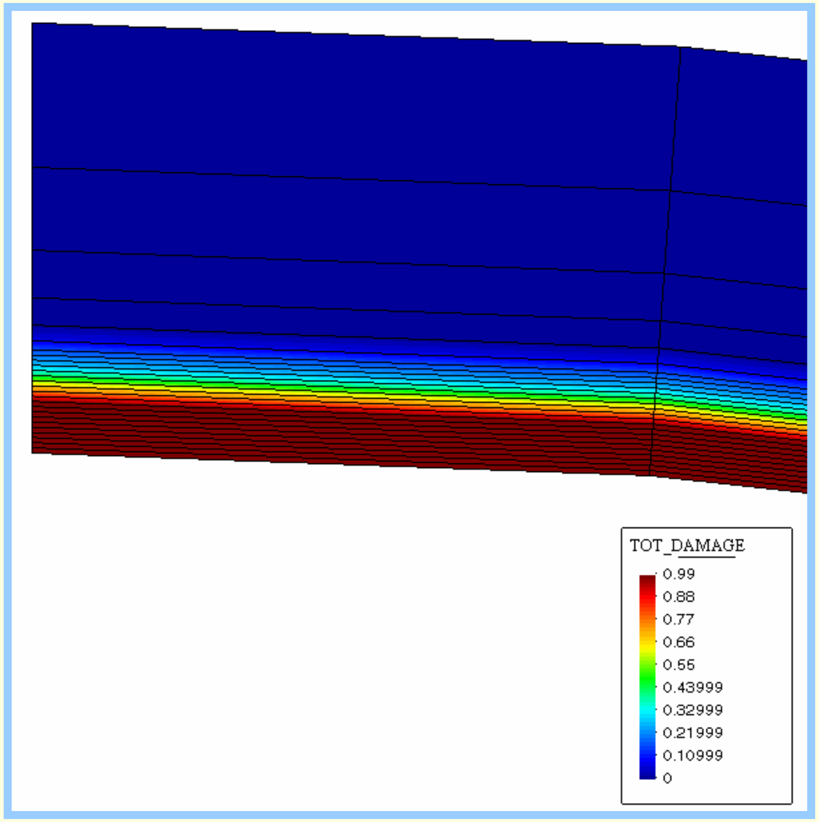

CONCLUSIONS

- The two chosen applications show that multi-disciplinary problems can be solved if high performance computing is consistently applied.
- However the collaboration of experts of the different involved fields is fundamental to obtain significant solutions.
- Scientific Computing can validly substitute expensive experiments